

# UWB ANTENNAS FOR BREAST & BRAIN TUMOR DETECTION USING MICROWAVE IMAGING

THESIS REPORT

Submitted by,

**ANJALY R**

**TKM21ECCS02**

to

the APJ Abdul Kalam Technological University in partial fulfillment of the  
requirements for the award of the Degree

of

Master of Technology

in

*Communication Systems*



DEPARTMENT OF ELECTRONICS AND COMMUNICATION  
ENGINEERING  
TKM COLLEGE OF ENGINEERING  
KOLLAM 691 005

May 2023

# UWB ANTENNAS FOR BREAST & BRAIN TUMOR DETECTION USING MICROWAVE IMAGING

THESIS REPORT

Submitted by,

**ANJALY R**

**TKM21ECCS02**

to

the APJ Abdul Kalam Technological University in partial fulfillment of the  
requirements for the award of the Degree

of

Master of Technology

in

*Communication Systems*

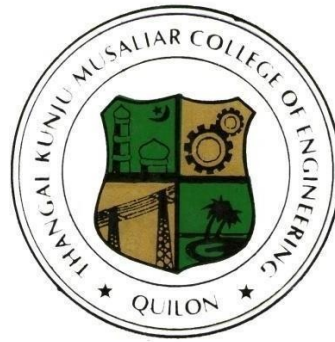


DEPARTMENT OF ELECTRONICS AND COMMUNICATION  
ENGINEERING  
TKM COLLEGE OF ENGINEERING  
KOLLAM 691 005

May 2022

**DEPARTMENT OF ELECTRONICS & COMMUNICATION  
ENGINEERING**

**TKM COLLEGE OF ENGINEERING  
KOLLAM 691 005**



**CERTIFICATE**

This is to certify that the thesis report entitled “**UWB ANTENNAS FOR BREAST & BRAIN TUMOR DETECTION USING MICROWAVE IMAGING**” is a bonafide report presented by **ANJALY R** in partial fulfilment of the requirement for the award of Master of Technology Degree in Communication Systems (Electronics and Communication Engineering) of APJ Abdul Kalam Technological University during the year 2022-2023.

**Project Guide,**  
**Dr.NISSAN KUNJU**  
Associate Professor  
Dept.of ECE  
TKMCE

**Project Coordinator,**  
**Dr.NISHANTH N**  
Professor  
Dept.of ECE  
TKMCE

**HOD,**  
**Prof.SHABEER S**  
Associate Professor  
Dept.of ECE  
TKMCE

## ACKNOWLEDGEMENT

At the outset, I consider it my duty to thank Almighty God for giving me the necessary wisdom to successfully complete this project presentation.

I thank **Prof.SHABEER S**, HOD, Department of Electronics and Communication, for his encouragement and support.

I express my sincere thanks to our Project coordinator, **Dr.NISHANTH N**, Professor, Department of Electronics and Communication Engineering, for the support and encouragement during the course of this presentation.

I take this opportunity to express my sincere gratitude and profound thanks to my Project guide, **Dr.NISSAN KUJU**, Associate Professor, Department of Electronics and Communication, for his advice, supervision and patience during the course of project preparation and presentation and for providing me guidance and critical inputs in the preparation and presentation of my project.

I express my sincere thanks to , **Dr.SUKOMAL DEY**, Assistant Professor,IIT Palakkad and **Mr.ATHUL O ASOK**, Research Scholar,IIT Palakkad, for the proper guideness and encouragement during the course of this presentaion of my project.

I would also like to express my sincere gratitude to all my teachers, friends and my parents for their much needed support during the preparation and presentation of the project.

**ANJALY R**

TKM21ECCS02

# ABSTRACT

In the last decades, microwave imaging has emerged as a new area of research due to its many advantages over current imaging systems. Microwave imaging system is used for indepth inspection of biological tissues. It aids in identification of morphological changes in these biological tissues, as well as their locations. The emerging Ultra Wideband (UWB) microwave imaging gives better result and has the advantage of using non-ionizing radiation. In these systems, antennas play a very important role. Antenna design optimization has gained significance because the device is placed close to the human body. This research introduces four compact antennas for tumor detection. Two for head imaging and two for breast imaging applications. All of them is build on FR4 material. First we designed a pentagonal patch antenna for breast imaging applications, in the frequency range from 2.9 - 13 GHz with 125 % fractional bandwidth (FBW) and has maximum gain of 2.80 dBi at 8.79 GHz. The second breast imaging antenna is a blade shape patch antenna has a broad bandwidth in the frequency range from 2.6 - 13.56 GHz with 136% FBW and has maximum gain of 6.28 dBi at 12.9 GHz. Third one is a flower shaped patch antenna for head imaging application in the frequency range of 1.59 to 6 GHz with 116.20 % FBW and has maximum gain of 4 dBi at 4.62 GHz. The last antenna which we have designed for head imaging application is a modified square patch antenna in the frequency of 1.99 to 7.45 GHz with 115.67 % FBW and has maximum gain of 3.4 dBi at 6 GHz. Here we use monostatic approach of breast and brain tumor detection. All the simulations are done using CST Microwave studio EM Solver, 2016. For detecting the presence of tumor we designed head and breast phantom model with tumor at the center of the phantom model using CST. The properties of phantom model are similar to human body. The signal that transmitted from the antenna will reach the phantom with tumor inside, the signal will reflect from the phantom are examined to find the presence of tumor. These electromagnetic waves are capable to penetrate biological tissue in a very efficient way and maintain a reasonable attenuation. The image that received are reconstructed using image reconstruction algorithms such as DAS and DMAS algorithm to find tumor location. And all the designed antenna are in acceptable SAR range according to FCC regulations.

# Contents

<b>List of Figures</b>	<b>v</b>
<b>List of Tables</b>	<b>vii</b>
<b>List of Abbreviations</b>	<b>viii</b>
<b>1 INTRODUCTION</b>	<b>1</b>
1.1 AIM & OBJECTIVES . . . . .	2
1.2 UWB ANTENNA BASED MICROWAVE IMAGING SYSTEM . . . . .	2
1.3 ORGANIZATION OF THE THESIS . . . . .	3
<b>2 LITERATURE REVIEW</b>	<b>4</b>
2.1 RESEARCH GAPS IDENTIFIED . . . . .	19
<b>3 ANTENNA DESIGN &amp; ANALYSIS</b>	<b>20</b>
3.1 CPW-FED PENTAGONAL PATCH ANTENNA FOR BREAST IMAG- ING . . . . .	20
3.2 BLADE SHAPED PATCH ANTENNA FOR BREAST IMAGING . . . . .	22
3.3 FLOWER SHAPED PATCH ANTENNA FOR HEAD IMAGING . . . . .	24
3.4 MODIFIED SQUARE SHAPED PATCH ANTENNA FOR HEAD IMAG- ING . . . . .	27
3.5 PERFORMANCE COMPARISON . . . . .	29
<b>4 SAR ANALYSIS</b>	<b>31</b>
4.1 PHANTOM DESIGN . . . . .	31
4.2 SAR VALUE DETECTION . . . . .	33

<b>5</b>	<b>TUMOR DETECTION</b>	<b>35</b>
5.1	ANTENNA INVESTIGATIONS IN DESIGNED PHANTOM ENVIRONMENT . . . . .	35
5.2	IMAGE RECONSTRUCTION OF TUMOR . . . . .	39
<b>6</b>	<b>CONCLUSION &amp; FUTURE SCOPE</b>	<b>41</b>
<b>7</b>	<b>PUBLICATIONS FROM THIS THESIS</b>	<b>42</b>
	<b>REFERENCES . . . . .</b>	<b>43</b>

# List of Figures

1.1	Tumor detection techniques . . . . .	2
2.1	Breast cancer statistics in 2020 [2] . . . . .	5
2.2	Number of new cancer cases in 2020 [3] . . . . .	5
2.3	(a) Breast phantom (b) Tumor made of wheat flour at center of breast phantom [10] . . . . .	7
2.4	SAR values on the breast phantom at (a) 5.7 GHz and (b) 6.5 GHz [10]	7
2.5	Simulation setup [13] . . . . .	8
2.6	Imaging results for (a), unhealthy breast and (b), healthy breast. [13]	8
2.7	Antenna placed in contact with the breast to different distances [15] .	9
2.8	(a) Breast phantom (b) Simulation setup for breast cancer imaging [16]	9
2.9	Geometry of the proposed antenna [18] . . . . .	10
2.10	Breast tissue model with the antenna element [21] . . . . .	11
2.11	Image reconstruction using DAS (left) and DMAS (right) algorithms with one spherical cancer model [21] . . . . .	11
2.12	Antenna array surrounding the breast model [22] . . . . .	12
2.13	The location of the tumor inside the breast phantom at 6.85 GHz. [22]	12
2.14	Brain Tumor Staistics [5] . . . . .	13
2.15	Antenna with (a) Phantom model of human head and (b) Angular view of the human head phantom model [27] . . . . .	15
2.16	SAR distribution for an input power of 2mW [30] . . . . .	15
2.17	(a) Monopole antenna printed on FR4 substrate. (b) Monopole antenna embedded into the brick. [33] . . . . .	16
2.18	CAD head phantom and brick antennas' configuration [33] . . . . .	17
2.19	Head phantom model layers [36] . . . . .	17

2.20	Near field directivity both for with and without tumor. [36] . . . . .	18
3.1	Geometry of the proposed CPW-fed pentagonal patch antenna . . . . .	21
3.2	S parameter plot of the proposed CPW-fed pentagonal patch antenna	21
3.3	Gain plot of the proposed CPW-fed pentagonal patch antenna . . . . .	22
3.4	3D radiation pattern of the proposed CPW-fed pentagonal patch antenna at 6 GHz . . . . .	22
3.5	Geometry of the proposed blade shaped patch antenna . . . . .	23
3.6	S parameter plot of the proposed blade shaped patch antenna . . . . .	23
3.7	Gain plot of the proposed blade shaped patch antenna . . . . .	24
3.8	3 D radiation pattern of the proposed blade shaped patch antenna at 11.36 GHz . . . . .	24
3.9	Geometry of the proposed flower shaped patch antenna . . . . .	25
3.10	S parameter plot of the proposed flower shaped patch antenna . . . . .	26
3.11	Gain plot of the proposed flower shaped patch antenna . . . . .	26
3.12	3D radiation plot of the proposed flower shaped patch antenna at 4.62 GHz . . . . .	27
3.13	Geometry of the modified square shaped patch antenna . . . . .	28
3.14	S parameter plot of the modified square shaped patch antenna . . . . .	28
3.15	Gain plot of the modified square shaped patch antenna . . . . .	29
3.16	3D radiation plot of the modified square shaped patch antenna at 4.62 GHz . . . . .	29
4.1	Breast phantom model . . . . .	32
4.2	Head phantom model . . . . .	32
4.3	SAR analysis of flower shaped patch antenna . . . . .	33
4.4	SAR analysis of modified square shaped patch antenna . . . . .	33
4.5	SAR analysis of CPW-fed pentagonal patch antenna . . . . .	34
4.6	SAR analysis of blade shaped patch antenna . . . . .	34
5.1	CPW-fed pentagonal patch antenna with breast phantom model . . . . .	36
5.2	S parameter plot of CPW-fed pentagonal patch antenna with breast phantom model . . . . .	36

5.3	Blade shaped patch antenna with breast phantom model . . . . .	37
5.4	S parameter plot of blade shaped patch antenna with breast phantom model . . . . .	37
5.5	Flower shaped patch antenna with head phantom model . . . . .	38
5.6	S parameter plot of flower shaped patch antenna with head phantom model . . . . .	38
5.7	Modified square shaped patch antenna with head phantom model . .	39
5.8	S parameter plot of modified square shaped patch antenna with head phantom model . . . . .	39
5.9	Breast image reconstruction using DAS algorithm . . . . .	40
5.10	Breast image reconstruction using DMAS algorithm . . . . .	40

# List of Tables

2.1	Patch antennas for breast tumor detection based on increasing order of fractional bandwidth percentage (FBW%) . . . . .	6
2.2	Patch antennas for brain tumor detection based on increasing order of fractional bandwidth percentage . . . . .	14
3.1	CPW-fed pentagonal patch antenna's functional parameters in mm . . . . .	20
3.2	Blade shaped patch antenna's functional parameters in mm . . . . .	23
3.3	Flower shaped patch antenna's functional parameters in mm . . . . .	25
3.4	Modified square shaped patch antenna's functional parameters in mm . . . . .	27
3.5	Patch antennas for breast tumor detection based on increasing order of fractional bandwidth percentage (FBW%) . . . . .	29
3.6	Patch antennas for brain tumor detection based on increasing order of fractional bandwidth percentage . . . . .	30
4.1	Properties of breast phantom model . . . . .	31
4.2	Properties of head phantom model . . . . .	33

# List of Abbreviations

<b>UWB</b>	Ultra Wide Band
<b>FBW</b>	Fractional Bandwidth
<b>CST</b>	Computer Simulation Technology
<b>DAS</b>	Delay and Sum
<b>DMAS</b>	Delay Multiply and Sum
<b>EM</b>	Electromagnetic
<b>SAR</b>	Specific Absorption Rate
<b>FCC</b>	Federal Communications Commission
<b>FR4</b>	Flame Retardant 4
<b>CAD</b>	Computer Aided Design
<b>CPW</b>	Co planar Waveguide
<b>MWI</b>	Microwave Imaging

# Chapter 1

## INTRODUCTION

The diseases that pose the greatest hazard to women are breast tumours. By 2035, there will be more than 25 million more different types of tumor cases [1-4], according to predictions. Unhealthy lifestyle and a growing population have both led to an increase in cancer cases. Breast cancer normally develops as a result of hormonal changes or the existence of malignant cells within breast tissue [1-4]. Similarly, one of the most lethal neurological conditions of the brain, is brain cancer which is brought on by malignant tumours inside the brain tissue [5-9]. Early detection and the right treatments can cure cancers. Earlier and accurate diagnosis of breast cancer is crucial for its successful treatment, according to prior study. The survival percentage for breast cancer might increase to 97% with early detection and treatment. This highlights the essential need for effective earlier cancer screening techniques.

There are different types of cancer detection techniques available now as shown in figure 1.1. Each one having its own advantages and disadvantages. Based on the disadvantages of available clinical screening techniques we are focusing on microwave imaging based on UWB antennas. The fundamental idea behind microwave imaging is to penetrate human tissue with microwave waves and then use the back scattered signal from human body, to detect changes in the tissue. Tumour cells inside the tissue have greater dielectric constants than normal tissues because of high water content. In microwave imaging systems, antenna's act as a sensors, since the antenna serves as both a transmitting and a receiving sensor. And they must have high gain, small in size, high fractional bandwidth percentage and also according to the Federal Communications Commission (FCC) has permitted commercial use of UWB bands

in the 7.5 GHz range (from 3.1 to 10.6 GHz) [1-9]

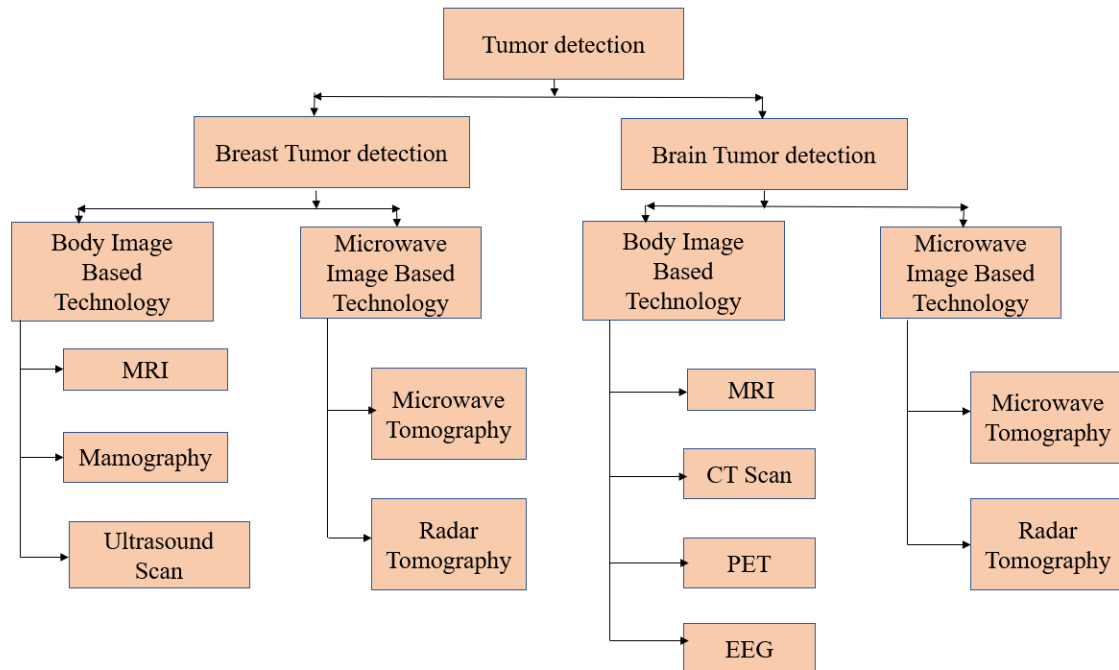


Figure 1.1: Tumor detection techniques

## 1.1 AIM & OBJECTIVES

The aim of our research is to design compact antennas for breast and brain tumor detection. In the microwave imaging system antenna plays a crucial role. The optimization in the field of antenna design are very much important. So our objective is to design an antenna having flexible and compact in size with UWB frequency range, the antenna must have high fractional bandwidth, high gain and also all the antenna must be in the acceptable SAR range according to FCC regulations

## 1.2 UWB ANTENNA BASED MICROWAVE IMAGING SYSTEM

Microwave (MW) imaging is the process of using electromagnetic fields at microwave frequencies between 300 MHz and 30 GHz to view an object's inside structure

[10-38]. Microwaves are transmitted from the transmitter through the phantom and are detected by a receiver that is placed on the opposite side or the same transmitter. When waves pass through a tumour in the breast or the brain, the waves undergo a shift; the incident wave is then scattered and reflected. The quantity of incident wave energy at the receiver is significantly impacted by this. Transceivers are used as antennas in microwave imaging (as a sensor). A UWB antenna has special characteristics like non contact distant operations, intrinsic electrical transducers, environmental friendliness, bio compatibility, and biological friendliness. It can operate in both low and high frequency ranges. For microwave imaging applications, researchers have suggested employing a variety of UWB antennas, including those with omnidirectional vs. directional emission patterns, vast ranges vs. limited bands, high vs. low frequency, etc. These systems must always have higher gains and efficiency with suitable penetration of human tissue. Many UWB antennas have been proposed to fulfil the necessary qualities.

In this research we designed for UWB patch antenna four tumor detection applications. Two for breast imaging and two for head imaging.

### **1.3 ORGANIZATION OF THE THESIS**

The structure of the thesis is shown below. Chapter 1 gives an overview of our project. Chapter 2 gives an idea about previous works associated with our projects and their limitations. Whereas chapter 3 deals with the antenna which we have designed and their analysis. We designed total four antenna for tumor detection applications. Two for breast imaging and two for head imaging. Chapter 4 discusses specific absorption rate analysis utilising the designed breast and brain phantom and the proposed antennas. Chapter 5 deals with tumor detection and image reconstruction algorithms. Chapter 6 draws the works to conclusion. Finally, chapter 7 gives the list of publications from this thesis

# Chapter 2

## LITERATURE REVIEW

The most frequent diagnosed issues in women is currently breast cancer, which has surpassed lung cancer globally [1]. In 2023, it is anticipated that 2,261,419 new cases of breast cancer in women would be discovered worldwide [1-3]. Beside skin cancer, breast cancer is the cancer that affects more women in the US than any other type. In the United States, 297,790 women are anticipated to receive an invasive breast cancer diagnosis in 2023, while 55,720 women are anticipated to receive a non-invasive breast cancer diagnosis. During the middle of the 2000s, invasive breast cancer in women has gone up by about 0.5% annually. This is presumably brought on by an increase in general female obesity, a decline in fertility rates and a rise in the average age of first pregnancies. Invasive breast cancer will be detected in 2,800 men in the US in 2023 [3]. In the United States, there are currently more than 3.8 million women who are coping with or have overcome breast cancer. In 2023, the number of breast cancer related deaths in the US is predicted to be 43,700 (43,170 women and 530 males). The fifth biggest cause of death in the world is female breast cancer. According to estimates, breast cancer will claim the lives of 684,996 women worldwide in 2025. Although in 1989, the number of women who have died from breast cancer has dropped by 43% since 2020. This is a result of earlier detection, better treatment and increased breast cancer awareness [2]. Consequently, over 460,000 breast cancer deaths were avoided during that time. Figure 2.1 depicted 2.3 million new cases reported in the year 2020 [2]. As per the Globocan data 2020, in India, breast cancer accounted for 13.5% (178361) of all cancer cases and 10.6% (90408) of all deaths (figure 2.2) [3]

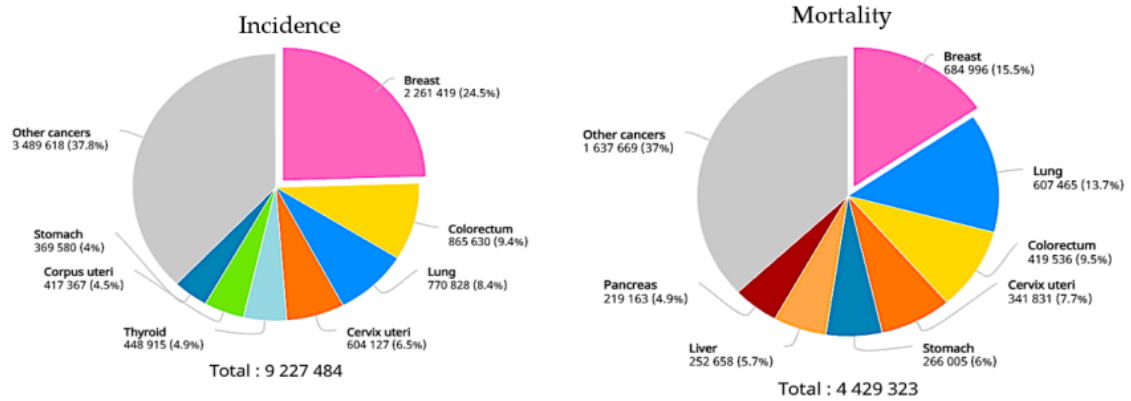


Figure 2.1: Breast cancer statistics in 2020 [2]

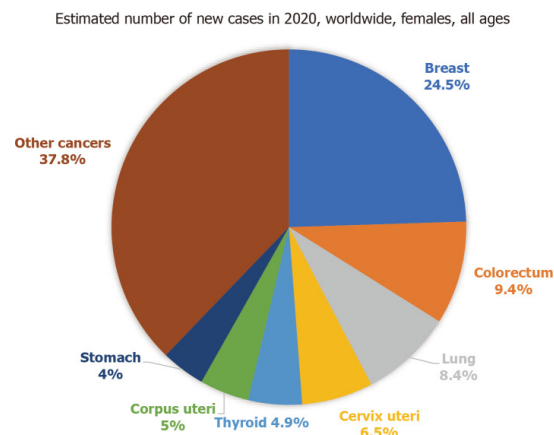


Figure 2.2: Number of new cancer cases in 2020 [3]

If a woman has a first degree family (mother, sister or daughter) who has been diagnosed with breast cancer, her risk of developing the disease practically doubles [2]. 15% of women who develop breast cancer have a family member who has been diagnosed with it. Between 5% and 10% of breast tumours have known gene alterations that can be passed down from one's mother or father. The most frequent gene mutations are in the BRCA1 and BRCA2 regions [1]. A BRCA1 mutation increases a woman's lifetime risk of breast cancer by up to 72%. Up to 69% of women are at risk if they carry a BRCA2 mutation. Breast cancer that has either a BRCA1 or BRCA2 mutation tends to strike younger women more frequently. Certain genetic variants are linked to an elevated risk of ovarian cancer. BRCA2 mutations in men increase their lifetime risk of developing breast cancer by about 6.8%, whereas BRCA1 mutations are a less common cause of breast cancer in men [1-3].

With the development of antenna systems, researchers looked closely at the creation of a whole microwave imaging system. This comprehensive survey is taken based on the fractional bandwidth percentage and the operating frequency of the designed antenna structure [10-26]. Table 3.5 shows the ascending order of fractional bandwidth percentage of several patch antennas for breast tumor detection.

Table 2.1: Patch antennas for breast tumor detection based on increasing order of fractional bandwidth percentage (FBW%)

PAP:	YR:	SUB:	DIM:(mm)	FRQ:(GHz)	FBW%	G.(dBi)
[10]	2019	FR-4	37 X 43 X 4.85	4.9-10.9	75.949	6.32
[13]	2022	FR-4	20 X 19 X 1.6	4-11GHz	93.33	3.05
[15]	2016	FR-4	25 X 16 X 0.8	4.23-11.71	93.851	4.55
[16]	2022	FR-4	18 X 28 X 1.6	3.4 -10	98.507	3.95
[17]	2022	FR-4	40 X 40 X 4	3.4-10.7	103.54	-
[18]	2016	FR-4	10.2 X 15.5 X 1.5	4.23-14	107.185	5.18
[21]	2020	FR-4	33.14 X 14.90 X 0.84	3.1-10.6	109.48	-
[22]	2016	FR-4	35 X 44 X 1.2	3.1-10.6	109.489	-
[26]	2016	FR-4	25 X 20 X 1.6	3.19-11.03	110.26	6

Kaur, et al. proposed the monostatic radar based technique to display microwave imaging of two spherical tumours of radii 4 and 5 mm in a breast phantom [10]. This is accomplished by using a three layered, stacked aperture coupled microstrip flawed grounded antenna structure with operating frequency of 4.9–10.9 GHz. The simulated peak gain of the proposed antenna, which has three layers and overall dimensions of 37 X 43 X 4.85  $mm^3$ , is 6.32 dBi at a frequency of 9.1 GHz with an impedance bandwidth of 6 GHz (4.9-10.9 GHz) and fractional bandwidth of 75.949%. A Vector Network Analyzer (VNA) and an anechoic chamber are used to verify the S parameters and gain results. Wheat flour, petroleum jelly, and polythene were used to create the breast phantom (with water as tumor) as shown in figure 2.3. Given that the antenna also exhibits simulated specific absorption rates of 0.27 and 1.115 W/Kg (on the breast phantom), respectively, for frequencies of 5.7 and 6.5 GHz, the suggested microwave technique is safe for human exposure (for 1 g of body tissue) as shown in figure 2.4.

Zerrad, et al. proposed a small UWB patch antenna with overall dimension of 20 X 19 X 1.6  $mm^3$  [13]. Slits are added to the patch and ground plane to change



Figure 2.3: (a) Breast phantom (b) Tumor made of wheat flour at center of breast phantom [10]

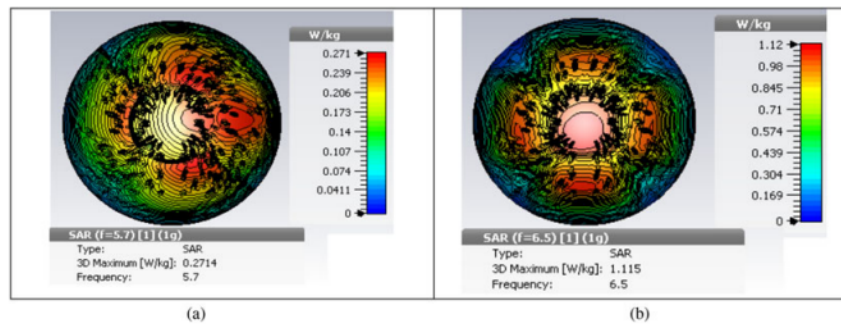


Figure 2.4: SAR values on the breast phantom at (a) 5.7 GHz and (b) 6.5 GHz [10]

the antenna thus it exhibit overall BW of 7 GHz (4-11 GHz) with more than 3 dBi gain. Antenna is made of FR-4 substrate, which has a loss tangent of 0.02 and a relative dielectric constant of 4.4 [14]. The antenna has a T-shaped slot ground plane and a rectangular patch with a step. The main goal of this research is to compare the back scattering signal with and without tumour. This set-up consists of two antennas pointing in the direction of the breast, a breast model with two layers breast tissue and skin and a tumour that is 6 mm inside the skin layer as shown in figure 2.5. Two antennas are placed facing and on the breast model's surrounding area at a distance of 12 mm from the skin layer to get the S parameters. The breast model is imaged both with and without a malignancy. A high resolution image can be used to determine the tumor's presence and location. The tumor's sensitivity is in Red, while the rest of the normal breast tissue is in Blue as shown in figure 2.6. When the tumour cell emits a higher signal than normal breast tissue, the scattering percentage of signals inside normal tissue is higher than that of tumours.

Karli, et al. proposed a miniature planar rectangular microstrip patch antenna on

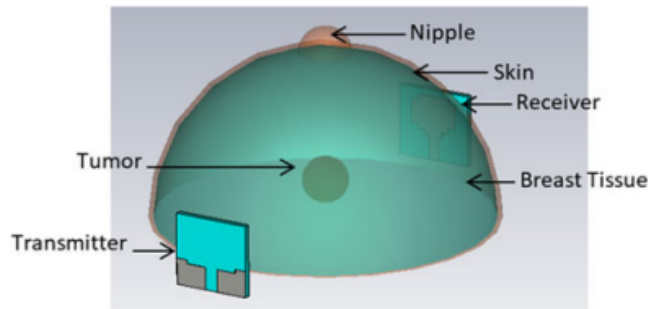


Figure 2.5: Simulation setup [13]

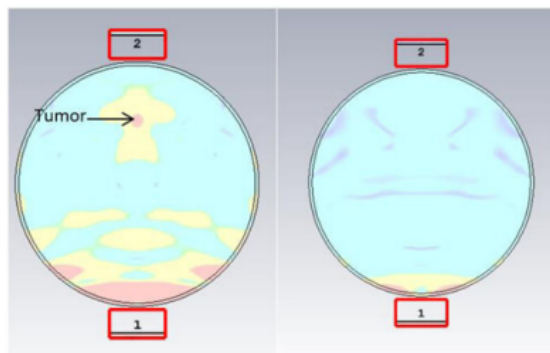


Figure 2.6: Imaging results for (a), unhealthy breast and (b), healthy breast. [13]

a FR4 epoxy substrate with dimension of  $25 \times 16 \times 0.8 \text{ mm}^3$  [15]. HFSS and CST were used to design, measure and simulate the proposed UWB antenna. The designed antenna operates at a range from 4.23 GHz to 11.71 GHz. Across the operational band, it was discovered that the antenna gain varied between 2.25dBi and 4.55 dBi, with an average radiation efficiency of 96%. The breast phantom model was designed as a cone shape with spherical tumor. Phantom comprises of skin and breast tissue as shown in figure 2.7

Ponnappalli, et al. proposed a circular slotted UWB antenna of  $18 \times 28 \text{ mm}^2$ , and its fractional bandwidth is 99% for the frequency range of 3.4 to 10 GHz [16]. The designed antenna was etched on a FR-4 substrate with a 4.3 relative permittivity, 0.002 loss tangent and 1.6 mm thickness. The recommended antenna has a maximum efficiency of 96.98%, excellent impedance matching and a sizable gain of 3.95 dBi. Authors concentrated on the creation of low profile, simple and high performance UWB antennas for the diagnosis of breast tumours. The detection of breast tumours can be practised

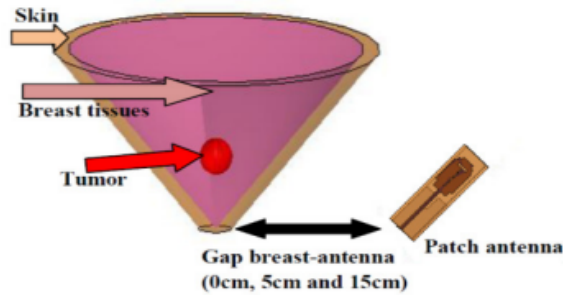


Figure 2.7: Antenna placed in contact with the breast to different distances [15]

on a breast phantom with two layers: skin and fat embedded with tumour. The designed antenna is then mounted 300mm apart from the breast phantom as shown in figure 2.8 for imaging.

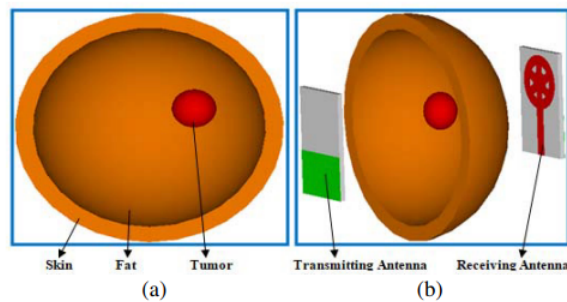


Figure 2.8: (a) Breast phantom (b) Simulation setup for breast cancer imaging [16]

A "C" shaped elliptically polarised DRA (dielectric resonator antenna) with an impedance bandwidth of 7.3 GHz (i.e., 3.4-10.7 GHz) covering the UWB was designed by Rai, et al. [17]. Wet etching and water jet cutting are used for the fabrication of the suggested DRA. Gelatin (skin), petroleum-jelly (fat), and wheat flour are used to create the physical model of the Bio medium (tumor) for imaging process. Using a vector network analyzer model number E5063A, the antenna radiation parameters are validated and good agreement between the results of the simulation and the measurements is seen. The size and identified location of tumour was detected by beamforming algorithm. By analysing the results the actual physical site of tumour with an error of 6.2% from the actual tumour location was found.

Gupta, et al. proposed an antenna, which is printed on FR4 substrate with a relative permittivity of 4.3 and a thickness of 1.5mm [18]. A radiating patch, a feed

network and a portion of a ground plane make up the antenna. Four identical unit cells are merged to create the radiating patch, which enables ultra wideband as shown in figure 2.9. The designed antenna with 10.2 mm x 15.5 mm dimension was operated throughout a frequency range of 4.23 to 14 GHz with gain levels up to 5.17 dB, radiation efficiency above 85% over the operational band, good fidelity up to 0.965 and the largest change in a group delay of 0.25 ns.

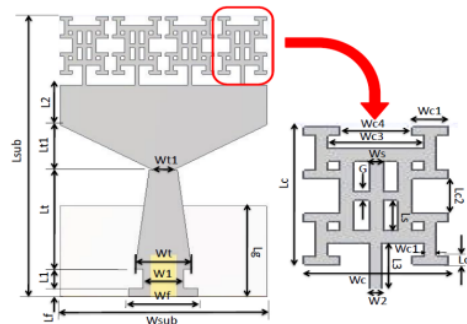


Figure 2.9: Geometry of the proposed antenna [18]

I.M.Danjuma. et al. shows a tiny slotted ultrawideband monopole antenna on FR4 substrate with overall dimension of  $33.14 \times 14.90 \times 0.84 \text{ mm}^3$ , which is then examined for bandwidth, gain, efficiency and radiation pattern both with and without the use of phantom model [21]. A good reflection coefficient ( $S_{11} -10 \text{ dB}$ ) is offered by the antenna in the UWB frequency range of 3.1 GHz to 10.6 GHz and gain of 4.71 dBi. The driven circular patch and four T-slots that are fused to form a quasi cross slot at the driven circular patch's centre make up the antenna construction. The proposed antenna is fed by a 50 ohm coaxial microstrip line. A three layer cylindrical breast tissue model were created to better understand the antenna performance as shown in figure 2.10. Designed antenna mounted with phantom model to analyse the tumor position and shape using delay-multiply-and-sum (DMAS) modified weighted delay and sum (MWDAS) reconstruction algorithms as shown in figure 2.11.

The S parameter plot obtained from UWB patch antenna is used to reconstructed using the Time Reversal MUSIC method [22]. The designed antenna and breast phantom have been chosen to operate within the range allocated by ISM (Industrial, Science and Medical) which is from 10 MHz to 20 GHz. With the aid of Matlab and CST

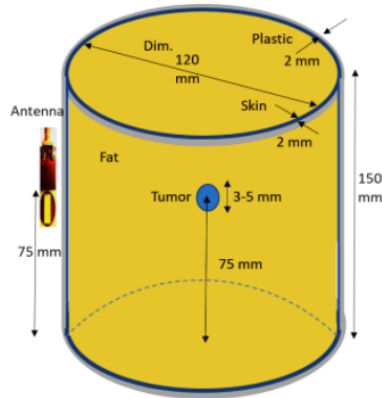


Figure 2.10: Breast tissue model with the antenna element [21]

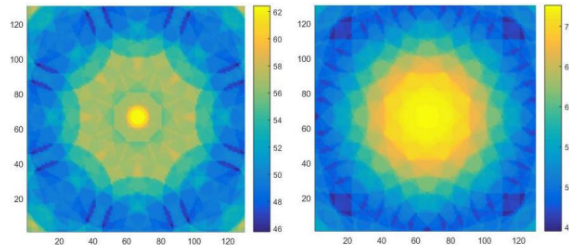


Figure 2.11: Image reconstruction using DAS (left) and DMAS (right) algorithms with one spherical cancer model [21]

Microwave Studio, all simulations were carried out. It uses the rectangular microstrip patch antenna on the top of an FR4 substrate having the overall dimensions of  $35 \times 40 \times 1.2 \text{ mm}^3$ , which is operating with an UWB range of 3.1-10.6 GHz frequency range. If an electromagnetic wave can propagate backward, it is referred to as time reversal since the signal would then refocus on the point source. The multi-static data matrix is used in TR microwave imaging techniques. Here, Bah, et al. suggest using the TR-MUSIC approach to locate a tumour in a breast phantom. The three components that make up the breast phantom are water, soy bean oil, and maize flour in the proportions of 6.5:2:1.5. Due to the high dielectric constant of malignant tissues in the case of breast cancer, mineral water has been taken into consideration, placed in a unit cell glass, and embedded in the phantom as shown in figure 2.12. Four antennas have been taken into consideration for our experimental study, and they have been symmetrically positioned around the pre designed breast phantom. The antennas are arranged in a 100 mm diameter circular. so that there are 200 mm between two

symmetric antennas. Figure 2.13 represents the location of tumor inside the breast phantom.

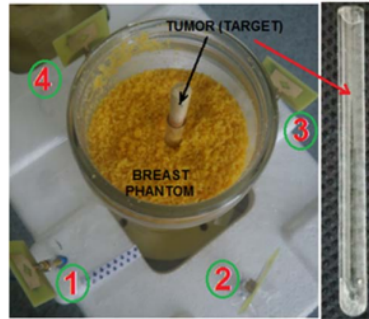


Figure 2.12: Antenna array surrounding the breast model [22]

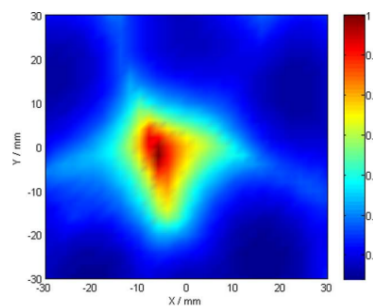


Figure 2.13: The location of the tumor inside the breast phantom at 6.85 GHz. [22]

M.Ojaroudi, et al. suggested a ground plane loop sleeve structure based monopole antenna for use in UWB applications using a FR4 substrate with overall dimension of  $25 \times 20 \times 1.6 \text{ mm}^3$  [26]. The antenna is made up of a ground planed pair of loop sleeves, a circular shaped tapered feed line and a rectangle radiating patch with a frequency of operation ranging from 3.19 to 11.03 GHz and it gives a fractional bandwidth of 110.26%.The effectiveness of the suggested antenna is good with averaging more than 85%. The gain level is acceptable, ranging from 4.5 to 6 dBi across the whole band.

A tumour that originates in the brain or spinal cord is called a primary brain or spinal cord tumour.A tumour that originates in the brain or spinal cord is referred to as a primary tumour. A primary malignant tumour of the brain or spinal cord will be identified in 24,810 adults (14,280 men and 10,530 women) in the US in 2023 [4]. Less

than 1% of people will experience this sort of tumour in their lives. 85% to 90% of all primary central nervous system tumours are brain tumours. In 2020, it is anticipated that 308,102 individuals will receive a primary brain or spinal cord tumour diagnosis worldwide [4-9].

In addition, 5,230 kids under the age of 20 are anticipated to receive a CNS tumour diagnosis in the US in 2023 [4-9]. There are secondary brain tumours or brain metastases in addition to primary brain tumours. This is when the tumour first appeared in the body and then metastasized to the brain. Leukaemia, lymphoma, melanoma, breast, kidney and lung cancers are the most typical cancers that move to the brain [4]. Only primary adult brain tumours are covered in this manual. The 10th biggest cause of death for both sexes is cancer of the neurological system, including the brain. In 2023, it is predicted that 18,990 people will die in the US from primary malignant brain and CNS tumours, including 11,020 males and 7,970 women [4]. According to estimates, primary malignant brain and CNS tumours claimed the lives of 251,329 people globally in 2020. Figure 2.14 shows the different brain tumor statistics [5]

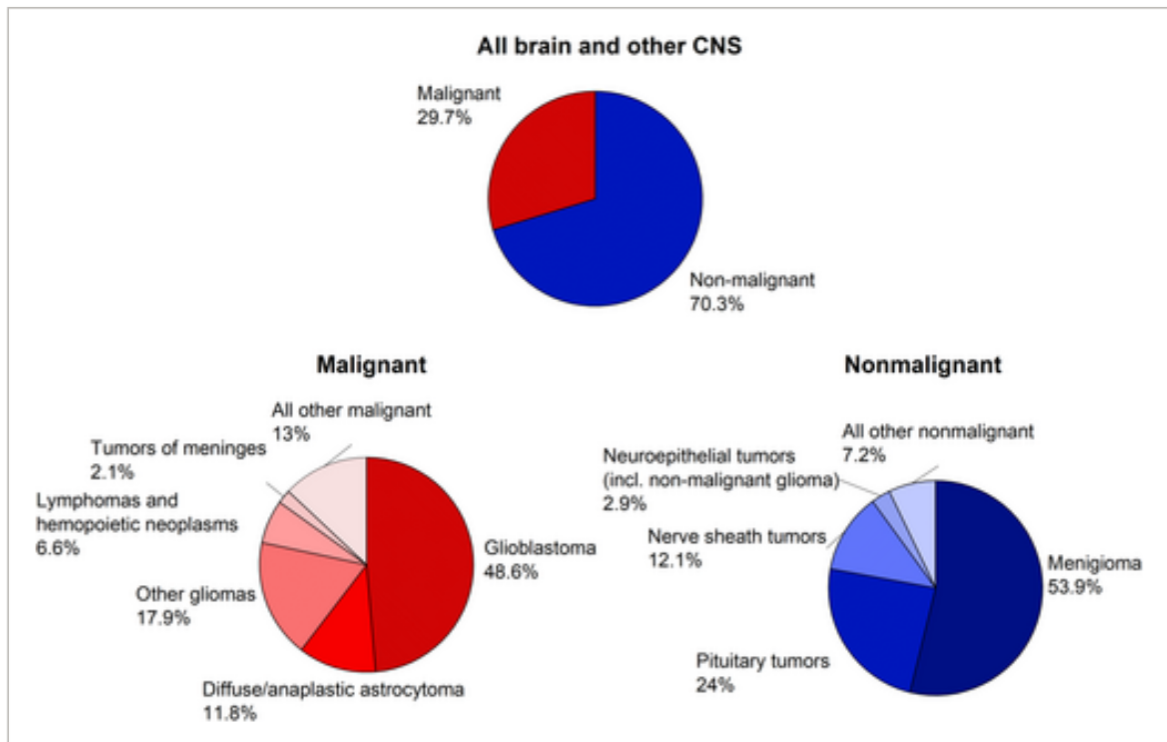


Figure 2.14: Brain Tumor Statistics [5]

Researchers analysed and find out that UWB patch antennas are the perfect solution for tumor detection. The comprehensive survey is taken based on the fractional bandwidth percentage and the operating frequency of the designed antenna structure [27-38]. Table 3.6 shows the ascending order of fractional bandwidth of several patch antennas for brain tumor detection.

Table 2.2: Patch antennas for brain tumor detection based on increasing order of fractional bandwidth percentage

<b>PAP:</b>	<b>YR:</b>	<b>DIM:(mm)</b>	<b>SUB:</b>	<b>FRQ:(GHz)</b>	<b>FBW%</b>	<b>G.(dBi)</b>
[27]	2018	29.99 X 29.99 X 0.59	FR4	0.908-0.928	2.178	-
[30]	2017	33 X 23 X 1	FR4	2.4-2.4835	3.419	-
[32]	2019	60 X 60 X 1.56	FR4	2.4-2.4835	3.419	-
[33]	2020	20 X 70 X 1.55	FR4	0.8-1.2	40	-
[34]	2019	68X 68X 12	FR4	1-1.7	51.85	-
[36]	2022	56 X 37 X 1.6	FR4	1.40-2.52	57.14	3.5
[37]	2016	20 X 80 X 1.6	FR4	1.1-2.2	66.6	3.15
[38]	2021	60.46 X 78.73 X 1.7	FR4	1.5-3	66.6	-

M.S. Bin Nesar, et al. proposed a body worn, single fed slotted T-shaped antenna that is primarily intended for use in the detection and localization of brain tumours that operates in the frequency range 902-928 MHz [27]. The antenna is fabricate on the top of an FR4 substrate with overall dimension of 29.99 X 29.99 X 0.59  $mm^3$ . The antenna was created in CST Microwave. It was then put over a complete human head phantom model made up of six separate layers. The layers are brain, cerebrospinal fluid, dura, skull, fat and skin respectively [29]. Under both normal and tumor affected settings, a number of performance assessments have been made, varying the tumor's position in relation to the antenna as shown in figure2.15. These data can be analysed to estimate the tumor's location. For the sake of the simulation, a tumour with a radius of 5 mm and conductivity and permittivity of 7 S/m and 55, respectively, has been considered. The proposed model's highest SAR was 0.332 W/ Kg, which complies with the necessary safety standards.

T.Cowdhury, et al. proposed an antenna that is a wearable with pentagon shaped micro strip patch for on body applications with 2.4 to 2.4835 GHz frequency [30]. It's small size makes it ideal for tumor detection. The dielectric substrate for the antenna is FR-4 lossy. Also, a human head phantom model with 5mm tumor is being created in order to obtain more idealised values for the antenna parameters [31]. The

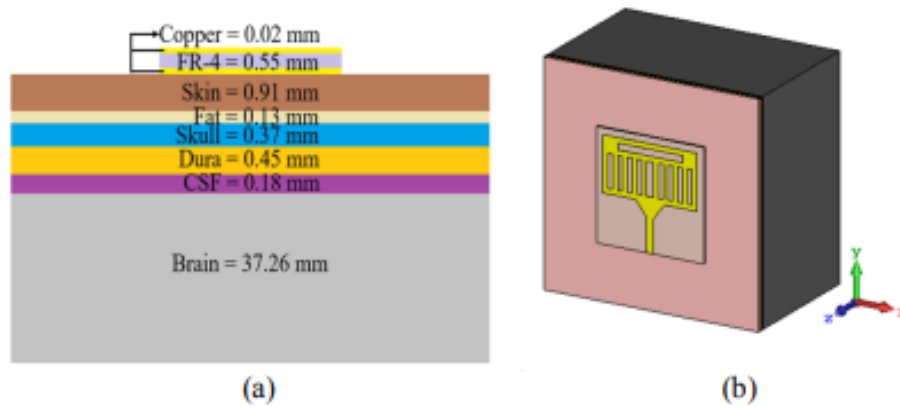


Figure 2.15: Antenna with (a) Phantom model of human head and (b) Angular view of the human head phantom model [27]

receiver antenna records the response after sending the input signal to the phantom model. The antenna continuously measures the radiation pattern, Voltage Standing Wave Ratio (VSWR) and Return loss of a head model with a normal head before contrasting these values with a head model with a benign tumour that is 5 mm in size. The brain's Specific Absorption Rate, which is suitable for human body use, should not exceed 1.6 W/kg according to IEEE standard safety regulations. The designed model's SAR was 0.36 W/kg as shown in figure 2.16.

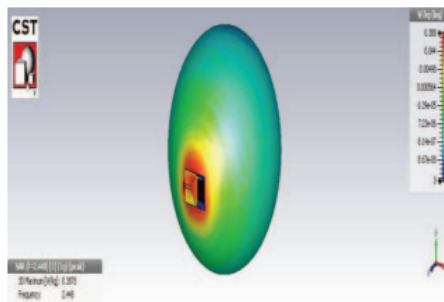


Figure 2.16: SAR distribution for an input power of 2mW [30]

M. J. Dishali, et al. proposed an rectangular microstrip patch antenna with overall dimensions of  $60 \times 60 \times 1.53 \text{ mm}^3$  [32]. It uses FR-4 as substrate since it is inexpensive and widely accessible. The created Patch antennas operate in the ISM band from 2.4-2.4835 GHz. The tumour is positioned in four different places on the human head phantom model, left side-top and bottom and right side-top and bottom. By rotating

the antenna array to scan the skull, the tumor's position can be found. The antenna's return loss on the brain phantom with the tumour is found to be -34.61GHz, which is higher than the return loss on the brain without the tumour. The specific absorption rate for 1gm of tissue was 0.0505W/kg, which is higher than the rate for brain tissue free of tumours.

D. O .Rodriguez, et al. suggested microwave antenna made specifically for an imaging system used to detect and track cerebrovascular diseases [33]. The antenna consists of a printed monopole submerged in a parallel block of semi flexible material with customised permittivity, avoiding the need for liquid coupling media and allowing for a straightforward array configuration. The "brick" is constructed from a compound of graphite powder and urethane rubber as in figure2.17. The proposed antenna operates in the frequency spectrum spans from 800 MHz–1.2 GHz.The antenna is constructed using a monopole antenna that was initially intended to function in a liquid coupling medium and was printed on a slab of ordinary FR4 (thickness: 1.55 mm, r: 4.4, and : 0.012 S/m). Finally, with an overall dimension of 20 X 70 X 1.5  $mm^3$ , it is tailored to work in a discrete coupling medium.Figure 2.18 shows a conventional anthropomorphic adult head is used as the basis for the computer aided design model of the human head for the numerical simulations . It can detect the presence of a spherical stroke area with a radius of 12.5 mm and has a sufficient EM wave penetration within the brain.

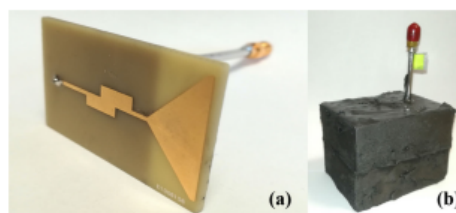


Figure 2.17: (a) Monopole antenna printed on FR4 substrate. (b) Monopole antenna embedded into the brick. [33]

M. Rokunuzzaman,et al. presented a small 3-D antenna with dimension of 68 X 68 X 12  $mm^3$  [34]. The antenna and the human head's homogeneity allow for more signal penetration for obtaining more useful data reflected from the brain.The designed antenna has a folded inverted F-like construction and a ground plane that is

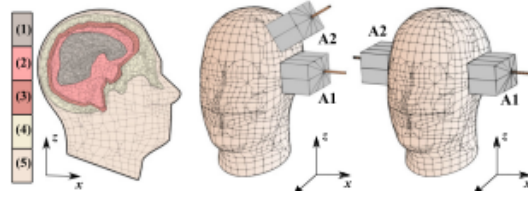


Figure 2.18: CAD head phantom and brick antennas' configuration [33]

loaded with slots. A rectangular cavity is built into the antenna's rear to reduce side and back lobe radiation. For the purpose of validating the antenna performance for use in medical diagnosis applications, a curved, homogeneous human head phantom was created. The designed antenna operates at a frequency range between 1 GHz and 1.7 GHz with 51.85% fractional bandwidth. Across the working frequency range, less than 0.0147 W/kg SAR is attained, which is lower.

Md. Mottahir Alam, et al. proposed a W-shaped slot loaded with solid U-shaped radiating patch and a slotted partial ground plane [36]. Efficiency, current distribution, gain and other antenna qualities have all been improved by the usage of slots with dimension of  $56 \times 37 \times 1.6 \text{ mm}^3$ . Patch was designed on a reasonably priced 1.6 mm thick FR4 substrate and a 50 ohm transmission line. The evaluated results showed that the specified prototype had omnidirectional radiation characteristics and a 1.12 GHz (1.40 - 2.52 GHz) bandwidth. The prototype offered a maximum radiation efficiency of 95% and a maximum gain of 3.5 dBi at 2.44 GHz with steady radiation characteristics. A head phantom model was created with 6 layers (figure 2.19). Figure 2.20 shows the near field directivity of antenna with and without tumour and the active bandwidth, the SAR value is limited to less than 0.3 W/kg.

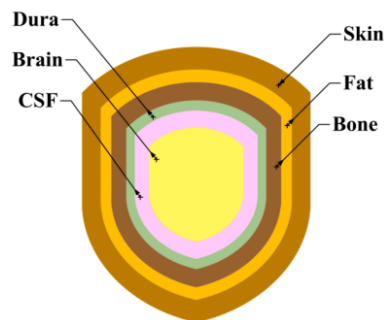


Figure 2.19: Head phantom model layers [36]

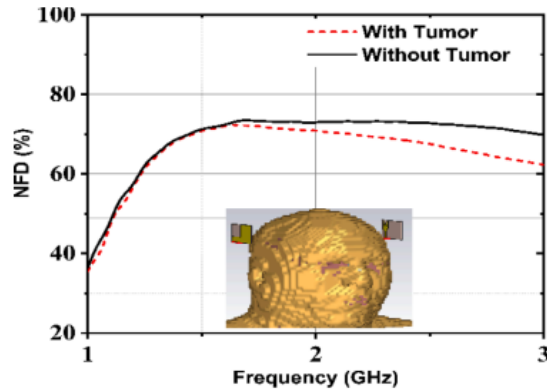


Figure 2.20: Near field directivity both for with and without tumor. [36]

A.T. Mobashsher, et al. designed an antenna with a slot loaded folded dipole construction with four furled sides that is supplied via a coplanar waveguide [37]. The antenna shows directed radiation in the frequency domain in both the near and far fields because to the greater currents on the top layer and reflections from the slightly extended bottom layer. With regard to the smallest working wavelength and 66.6% fractional bandwidth over 1.1-2.2 GHz, the antenna is small and low profile. Two printed dielectric blocks, two copper side walls and four furled copper plates make up the antenna. The antenna's top and bottom layers are printed on FR4, with thickness of 1.6 mm. The fundamental dipole and L-shaped furled copper plates connected to the dipole are divided by two U-shaped slots that are loaded into the top layer of the antenna. A 16-element antenna array is evaluated in a realistic simulation environment to determine a safe radiation exposure level because the antenna is intended to work inside an array for head imaging.

Due to small tumour size and several drawbacks of the methods employed for its identification make it challenging to pinpoint its location at an early stage. For this reason, S.A. Kadir, et al. suggested a rectangular microstrip patch antenna with a frequency range of 1.5 GHz to 3 GHz at a resonant frequency of 2.3 GHz (5G-Band) [38]. The Antenna was created using a FR-4 substrate material. The dimensions of the antenna used in this study are  $60.46 \times 78.73 \times 1.7 \text{ mm}^3$  and the feedline that fed the antenna's radiating patch is rectangular in shape. The CST Studio software was used to generate the human head phantom. To assess the antenna's effectiveness, it was used in the brain phantom both with and without a tumour. After using the

antenna in the brain phantom with and without the tumour, a reflection factor of -30.76 dB and -30.88 dB, respectively, was likewise attained.

## 2.1 RESEARCH GAPS IDENTIFIED

From this literature review it is evident that most of the antennas have the scope to improve its size, frequency of operation, gain and fractional bandwidth percentage. Due to this low frequency range the resolution of image will be less. And also due to less FBW the electromagnetic signal will does not deeply penetrate into the biological tissue. Hence tumor identification is very much difficult. The substrate used in these structure having large thickness value, hence the antennas are rigid not flexible. Hence they are difficult to handy due large dimensions.

Hence these works paved the way to design the antennas, that having compact in size with large UWB frequency of operation, high gain and high fractional bandwidth percentage.

# Chapter 3

## ANTENNA DESIGN & ANALYSIS

### 3.1 CPW-FED PENTAGONAL PATCH ANTENNA FOR BREAST IMAGING

The suggested breast imaging antenna is displayed in figure 3.1. Here, the antenna is fed by a rectangular microstrip feed line of dimensions  $B \times D$ . The feed line directly attached to a pentagonal patch of sides  $A$ . In the ground plane, initially, a CPW fed rectangular ground formed. The rest of the parametric values of the proposed antenna is given in the table 3.1.

Table 3.1: CPW-fed pentagonal patch antenna's functional parameters in mm

W	L	A	B	C	D	E	F
30	24	11.29	11.98	4.52	2.50	1	1

The ground plane is at a distance of 0.23 mm from the feed line. From this rectangle ground, based on the dimensions E,F,G,H and I, a stair case structure is etched out. This modified ground plane increases the performance of the designed structure. The entire structure is made on an FR4 structure of thickness 1.6 mm. The complete designed antenna is of dimension  $L \times W$ . The antenna has a bidirectional radiation pattern. Thus, to enhance the directionality of the antenna and to make is functional for biomedical imaging applications.

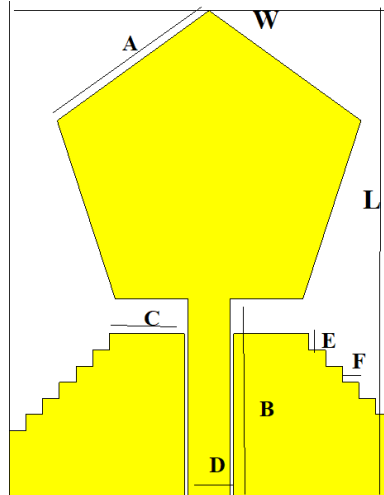


Figure 3.1: Geometry of the proposed CPW-fed pentagonal patch antenna

The return loss of the designed antenna is displayed in figure 3.2. It can be observed that the designed antenna works from 2.9 to 13 GHz with good impedance matching performance and fractional bandwidth of 125%. Figure 3.3 depicts the gain plot of the developed antenna. It can be understood that the gain of 2.80 dBi is obtained at 8.79 GHz.

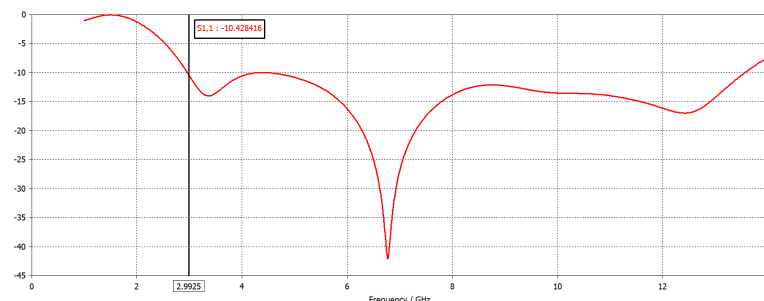


Figure 3.2: S parameter plot of the proposed CPW-fed pentagonal patch antenna

The 3D radiation pattern of the designed structure is extracted from the simulator and is displayed in figure 3.4. The radiation pattern at several frequencies like 4, 6.7, 8 and 9 GHz is observed. It can be observed that the proposed structure obtains directional radiation pattern at these frequencies. The directional radiation pattern along with broad band response is crucial for breast imaging applications. Computer Simulation Technology (CST) Microwave Studio 2016, an Electro Magnetic (EM) solver is used for all the simulations.

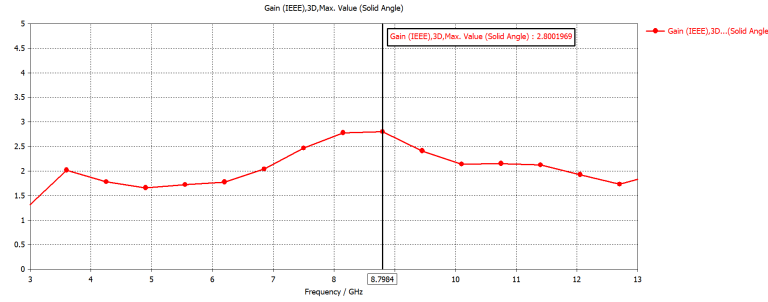


Figure 3.3: Gain plot of the proposed CPW-fed pentagonal patch antenna

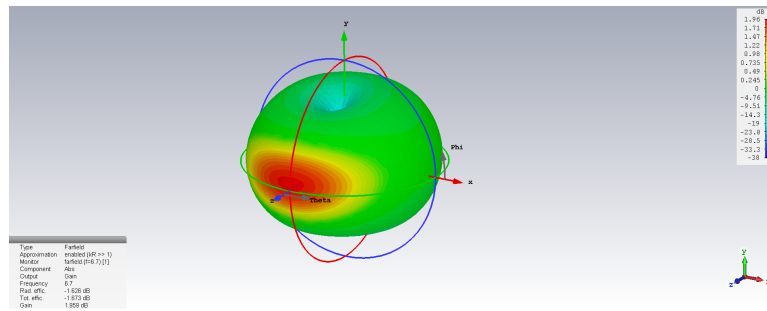


Table 3.2: Blade shaped patch antenna's functional parameters in mm

W	L	A	B	C	D	E	F	G	H	I	J	K
30	30	6.70	12.20	6	4	1	1	6.90	2.50	13.80	4	2.50

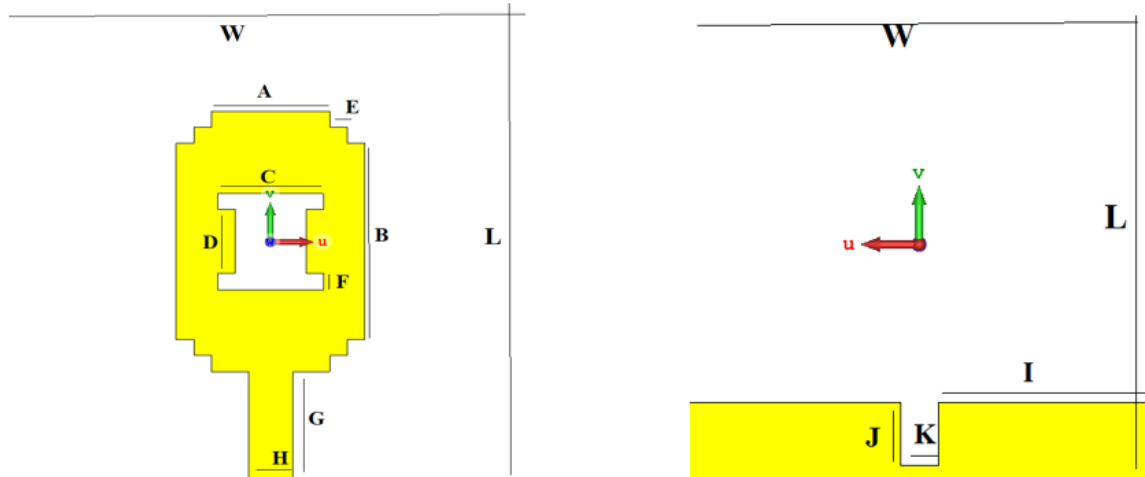


Figure 3.5: Geometry of the proposed blade shaped patch antenna

The simulated results of reflection coefficient ( $S_{11}$ ) for the above mentioned proposed antenna is depicted in figure 3.6. This blade shaped patch antenna operates at a frequency of 2.6 to 13.56 GHz with 136 % FBW. The simulated gain of monopole antenna is illustrated in figure 3.7. For entire operating bandwidth, the antenna simulated gain of 6.28 dBi at 12.9 GHz. From the figure 3.7 it is evident that gain increases linearly with frequency.

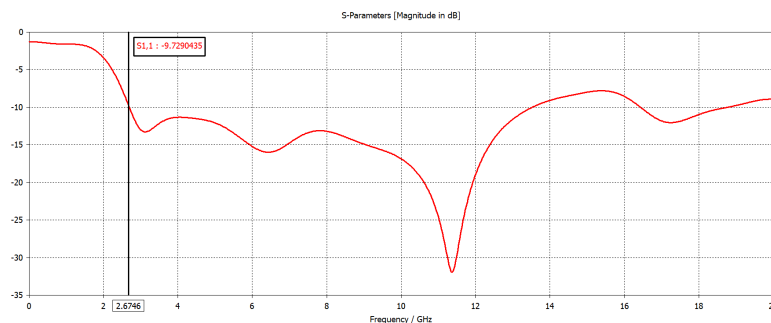


Figure 3.6: S parameter plot of the proposed blade shaped patch antenna

The 3D radiation pattern of the designed structure is extracted from the simulator and is displayed in figure 3.8. It can be observed that the proposed structure obtains

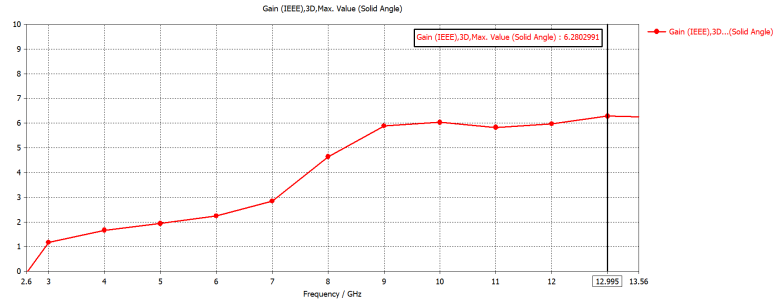


Figure 3.7: Gain plot of the proposed blade shaped patch antenna

directional radiation pattern at 11.36 GHz.

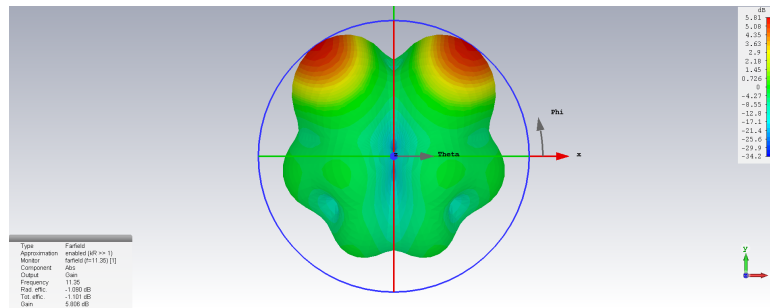


Figure 3.8: 3 D radiation pattern of the proposed blade shaped patch antenna at 11.36 GHz

### 3.3 FLOWER SHAPED PATCH ANTENNA FOR HEAD IMAGING

The complete geometry of the proposed head imaging antenna is displayed in figure 3.9. The front and back view of the designed antenna is displayed in figure 3.9. Initially an ellipse of major axis  $a$  and minor axis  $b$  is designed in the simulator. Four separate copies of the designed structure is made, each copy separated by 45 degree with respect to the ellipse center to form the flower shaped structure as displayed in the figure. Also, the minor axis  $b$  is parametrically optimized to get the best impedance matching performance. Further, a circular ring is placed around the flower shaped structure. This structure is designed by initially designing a circle of radius  $R_A$  and  $R_B$ . Then, the circle formed by  $R_B$  is etched out from the circle formed by  $R_A$  to get the ring design. Two slots of dimensions  $L_S \times W_S$  is also cut out

from the ring on either side of the feed structure, to obtain a very good impedance matching performance. The antenna is fed by a feed line of dimension  $L_F \times W_F$  to match the 50 ohm characteristic impedance. The back view of the designed antenna is also displayed in figure 3.9. Here, a copper layer of dimension  $L \times W$  is initially designed. This is followed by etching out a slot of dimension  $L_G \times W_G$ , to form the final structure. The entire structure is designed on a FR4 substrate of dimensions  $L \times W$ , with dielectric constant 4.4, loss tangent 0.025 and having thickness of 1.6 mm. All the final optimized dimensions of the designed antenna are tabulated and displayed in Table 3.3 for completeness.

Table 3.3: Flower shaped patch antenna's functional parameters in mm

$W$	$L$	$R_A$	$R_B$	$a$	$b$	$L_S$	$W_S$	$L_F$	$W_F$	$L_G$	$W_G$
50.4	33.3	10.6	10.2	20.4	10	0.47	0.27	10.7	2.7	24.3	31.5

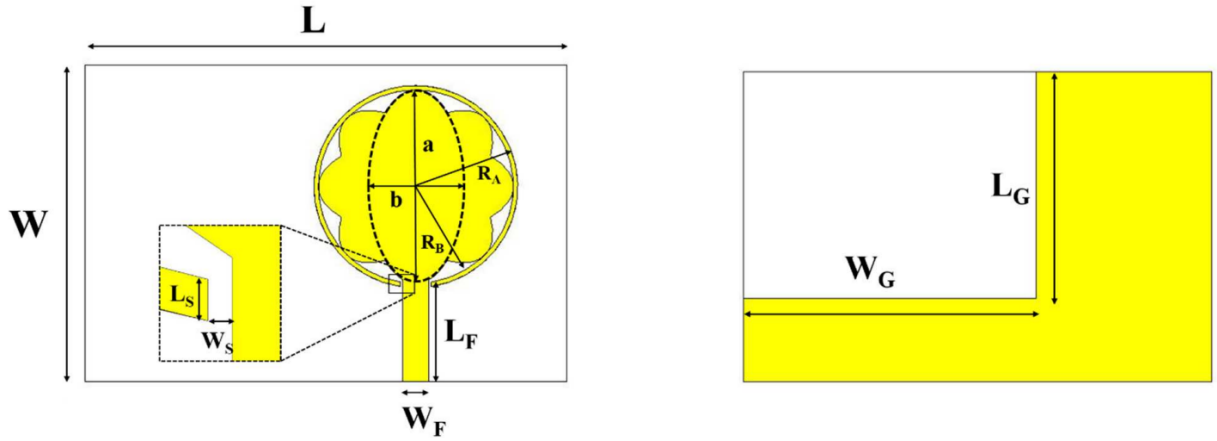


Figure 3.9: Geometry of the proposed flower shaped patch antenna

The simulated return loss of the proposed antenna is plotted and displayed in figure 3.10. It can be observed that the proposed antenna operates from 1.59 GHz to 6 GHz with a return loss greater than 10 dB. The antenna also attains a fractional bandwidth of 116.20%. The gain plot of the designed antenna is displayed in figure 3.11. It can be observed that the proposed antenna achieves a peak gain of 4 dBi which is the highest reported peak gain among the compact antennas used currently for head imaging applications.

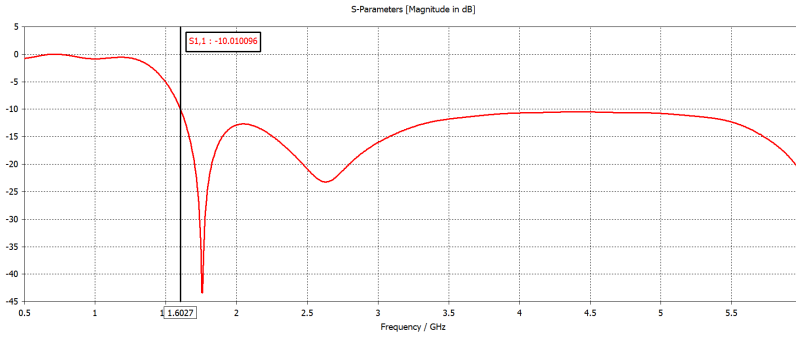


Figure 3.10: S parameter plot of the proposed flower shaped patch antenna

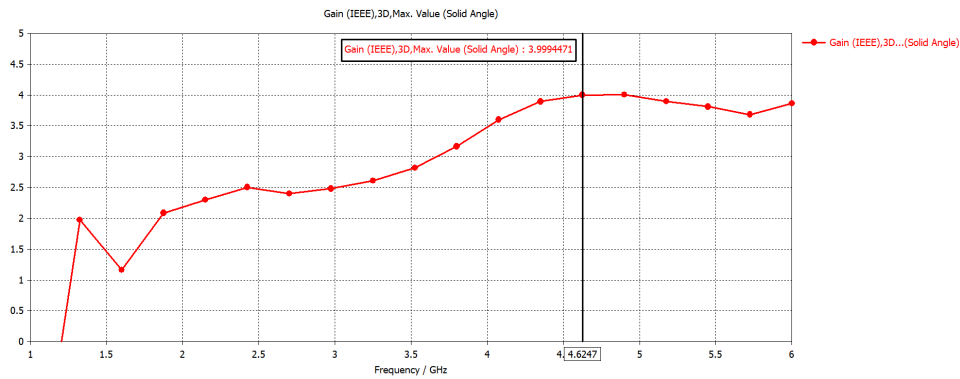


Figure 3.11: Gain plot of the proposed flower shaped patch antenna

The 3D radiation pattern of the designed antenna is displayed in figure 3.12. The radiation pattern at 2 GHz, 3 GHz, 4 GHz, 4.62 GHz and 5 GHz are plotted and observed. It can be observed that the designed antenna is directional at these frequencies. The performance of the proposed antenna is compared with similar antennas utilized for head imaging applications. It is observed that the proposed antenna obtains higher gain, higher bandwidth percentage, as well as maintains a compact size as compared to the other works in literature. All the simulations are carried out in the Finite Integration Technique (FIT) based EM solver Computer Simulation Technology (CST), 2016.

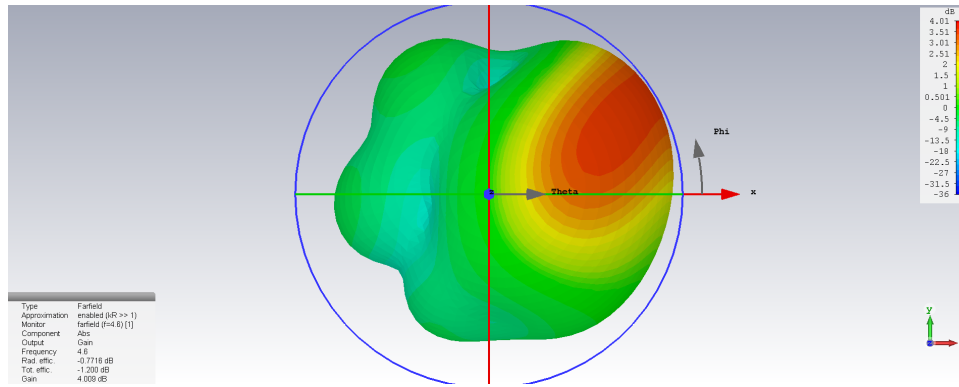


Figure 3.12: 3D radiation plot of the proposed flower shaped patch antenna at 4.62 GHz

### 3.4 MODIFIED SQUARE SHAPED PATCH ANTENNA FOR HEAD IMAGING

The proposed head imaging monopole antenna can transmit and receive signals with a frequency range of 1.99–7.45 GHz with 115.67 % FBW. The radiating patch incorporates a circular slot in the center and a tiny triangular cut at four corners. It is installed on a low cost FR4 epoxy substrate, with a loss tangent of 0.02 and a dielectric constant of 4.4. A microstrip line with a 50 ohm impedance supplies power to the antenna. As seen in figure 3.13 there are three notch in the patch to improve the match. The radiating patch is square with a circle and two semicircular cut out of the center, reducing the resonance size required at the working frequency. The cut off corner results in coupling between horizontal and vertical polarized modes. Other functional parametric values of this antenna is given in the table 3.4

Table 3.4: Modified square shaped patch antenna's functional parameters in mm

A	B	C	D	E	F	G	H	I	J
50	70	17	8.31	10	17	21	2.90	36	9.90

The simulated return loss of the proposed antenna is plotted and displayed in figure 3.14. It can be observed that the proposed antenna operates from 1.77 GHz to 7.45 GHz with a return loss greater than 10 dB. The antenna also attains a fractional bandwidth of 115.67%. The gain plot of the designed antenna is displayed in figure 3.15. It can be observed that the proposed antenna achieves a peak gain of 3.4 dBi

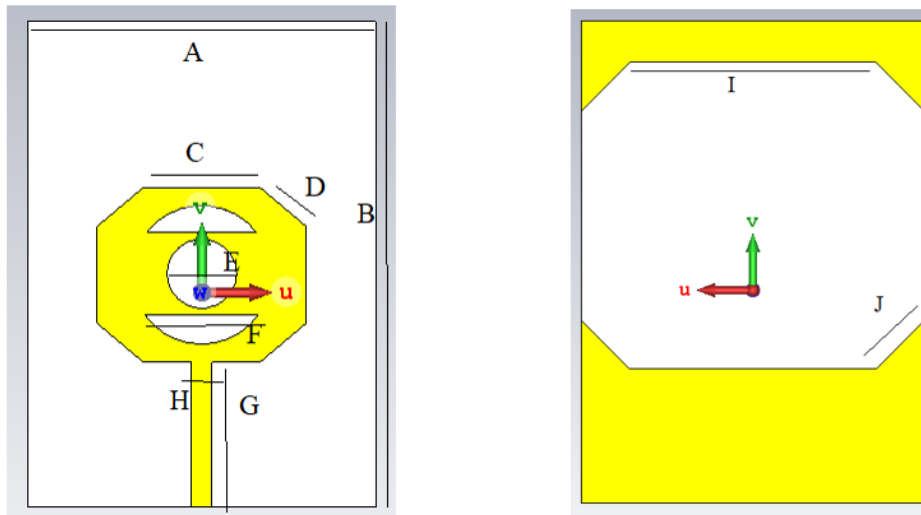


Figure 3.13: Geometry of the modified square shaped patch antenna

which is the highest reported peak gain among the compact antennas used currently for head imaging applications.

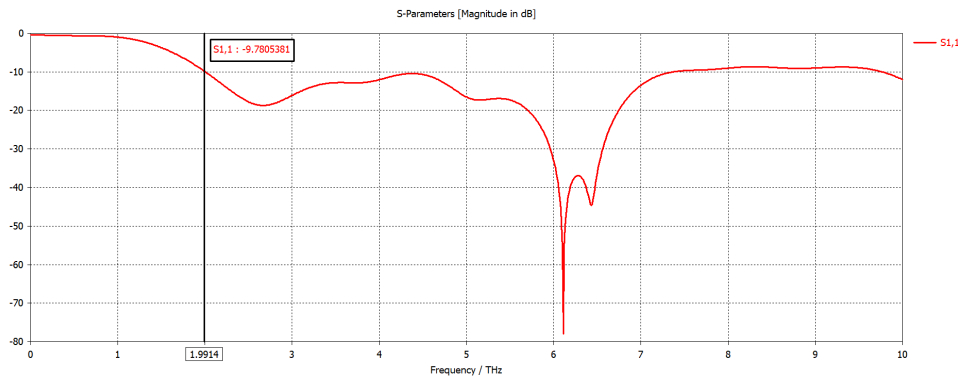


Figure 3.14: S parameter plot of the modified square shaped patch antenna

The 3D radiation pattern of the designed antenna is displayed in figure 3.16. The radiation pattern at 6 GHz are plotted and observed. It can be observed that the designed antenna is directional at this frequency. It is observed that the proposed antenna obtains higher gain, higher bandwidth percentage, as well as maintains a compact size as compared to the other works in literature. All the simulations are carried out in the Finite Integration Technique (FIT) based EM solver Computer Simulation Technology (CST), 2016.

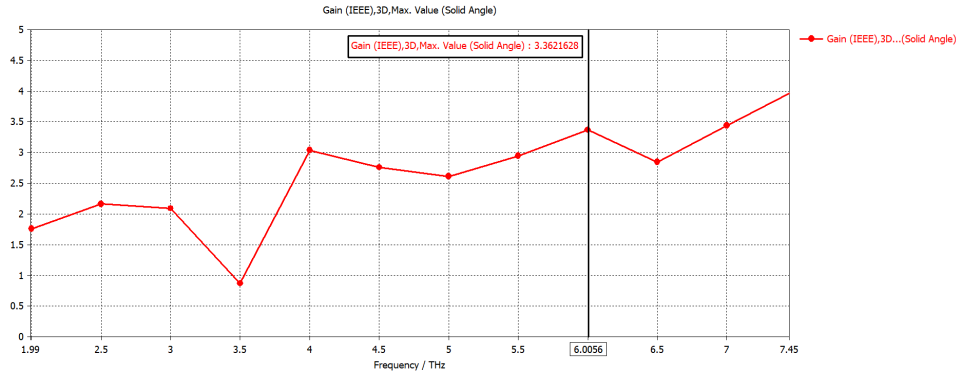


Figure 3.15: Gain plot of the modified square shaped patch antenna

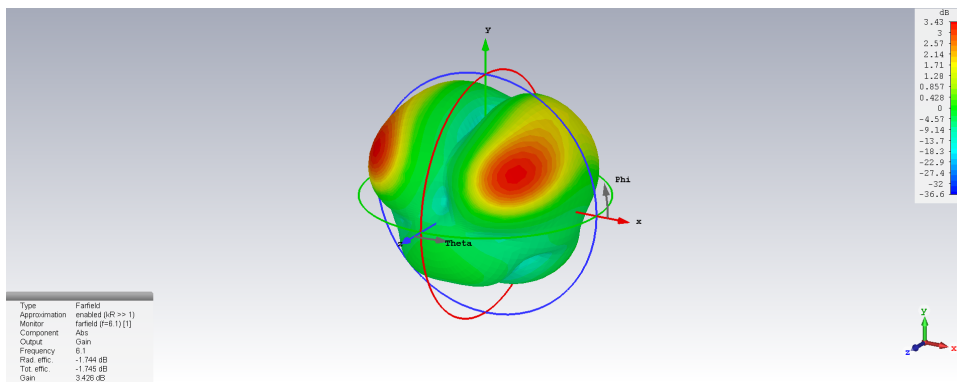


Figure 3.16: 3D radiation plot of the modified square shaped patch antenna at 4.62 GHz

### 3.5 PERFORMANCE COMPARISON

Table 3.5: Patch antennas for breast tumor detection based on increasing order of fractional bandwidth percentage (FBW%)

PAP:	YR:	SUB:	DIM:(mm)	FRQ:(GHz)	FBW%	G.(dBi)
[10]	2019	FR-4	37 X 43 X 4.85	4.9-10.9	75.949	6.32
[13]	2022	FR-4	20 X 19 X 1.6	4-11GHz	93.33	3.05
[15]	2016	FR-4	25 X 16 X 0.8	4.23-11.71	93.851	4.55
[16]	2022	FR-4	18 X 28 X 1.6	3.4 -10	98.507	3.95
[17]	2022	FR-4	40 X 40 X 4	3.4-10.7	103.54	-
[18]	2016	FR-4	10.2 X 15.5 X 1.5	4.23-14	107.185	5.18
[21]	2020	FR-4	33.14 X 14.90 X 0.84	3.1-10.6	109.48	-
[22]	2016	FR-4	35 X 44 X 1.2	3.1-10.6	109.489	-
[26]	2016	FR-4	25 X 20 X 1.6	3.19-11.03	110.26	6
<b>Pentagonal</b>	2023	FR-4	30 x 24 x 1.6	2.9 -13	125	2.6
<b>Blade</b>	2023	FR-4	30 x 30 x 1.59	2.6 -13.56	136	6.28

As compared to the previously proposed antennas for breast and brain tumor

Table 3.6: Patch antennas for brain tumor detection based on increasing order of fractional bandwidth percentage

<b>PAP:</b>	<b>YR:</b>	<b>DIM:(mm)</b>	<b>SUB:</b>	<b>FRQ:(GHz)</b>	<b>FBW%</b>	<b>G.(dBi)</b>
[27]	2018	29.99 X 29.99 X 0.59	FR4	0.908-0.928	2.178	-
[30]	2017	33 X 23 X 1	FR4	2.4-2.4835	3.419	-
[32]	2019	60 X 60 X 1.56	FR4	2.4-2.4835	3.419	-
[33]	2020	20 X 70 X 1.55	FR4	0.8-1.2	40	-
[34]	2019	68X 68X 12	FR4	1-1.7	51.85	-
[36]	2022	56 X 37 X 1.6	FR4	1.40-2.52	57.14	3.5
[37]	2016	20 X 80 X 1.6	FR4	1.1-2.2	66.6	3.15
[38]	2021	60.46 X 78.73 X 1.7	FR4	1.5-3	66.6	-
<b>Flower</b>	2023	33 x 50.4 x 1.6	FR-4	1.59 -6	116.2	4
<b>Square</b>	2023	50 x 70 x 1.5	FR-4	1.99 -7.45	115.67	3.36

detection, all the newly designed antennas have compact in size,high frequency of operation,large fractional bandwidth and high gain value.

# Chapter 4

## SAR ANALYSIS

### 4.1 PHANTOM DESIGN

The antenna has been evaluated for actual implementation capabilities in biomedical applications. The SAR reading is the decisive aspect that determines its practical utility for biomedical applications. According to the Federal Communication Commission (FCC), the globally acceptable estimate for SAR is 1.6 W/Kg when it is averaged over 1 g of tissue. In this work, a hemispherical breast phantom with an embedded tumor is modelled in CST. At first, the skin layer is made. The designed skin section is having a radius of 60 mm with 4 mm thickness. The fat layer is of radius 56 mm, fibroglandular layer having the radius of 50 mm and the tumor is embedded in the hemispherical phantom model's center position. The tumor is having a radius of 10 mm. The properties of all the layers are given in the table 4.1. The tumor is defined as a new material with permittivity of 54.9 F/m, conductivity of 4 S/m and density of 1058 Kg/m<sup>3</sup>. The modelled breast phantom with complete labelling is clearly displayed in figure 4.1.

Table 4.1: Properties of breast phantom model

Tissue	Permittivity(F/m)	Conductivity(S/m)	Density(Kg/m <sup>3</sup> )
Skin	36.7	2.34	1109
Fat	14.5	0.262	911
Fibroglandular	34	1.55	999
Tumor	54.9	4	1058

Similarly a spherical seven layered head model is designed in the simulator to

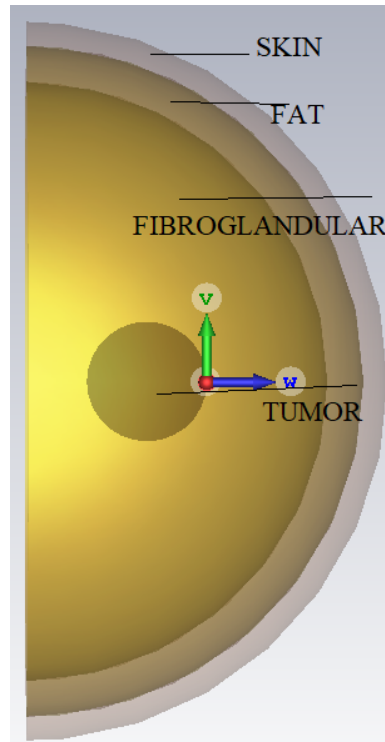


Figure 4.1: Breast phantom model

study the effect of the designed antenna on the human head as displayed in figure 4.2. The properties of all the layers are given in the table 4.2

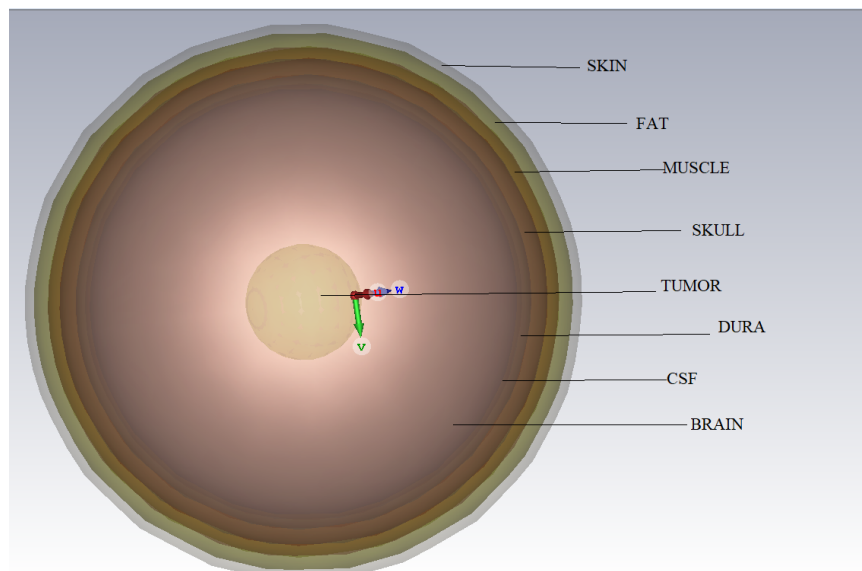


Figure 4.2: Head phantom model

Table 4.2: Properties of head phantom model

Tissue	Permittivity(F/m)	Conductivity(S/m)	Density(Kg/m <sup>3</sup> )
Skin	36.7	2.34	1109
Fat	14.5	0.262	911
Muscle	50	1.81	1090
Skull	15	0.59	1900
Dura	42.03	1.66	1041
CSF	66.2	3.45	1007
Brain	42.5	1.51	11400
Tumor	54.9	4	1058

## 4.2 SAR VALUE DETECTION

The first head imaging antenna called flower shaped patch antenna has obtained SAR of 0.0144 W/Kg ,which is very much less than the acceptable range as shown in figure 4.3. The antenna is placed at a distance of 150 mm from the phantom center.

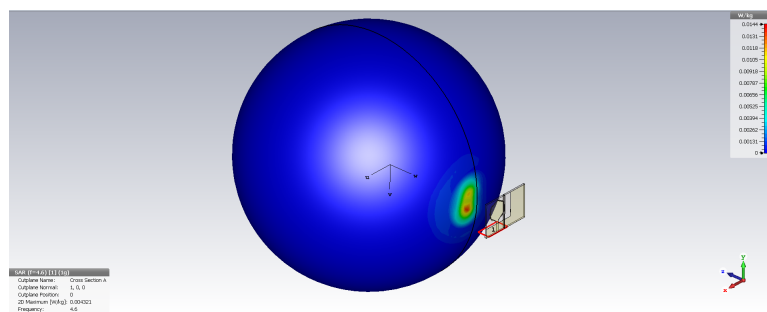


Figure 4.3: SAR analysis of flower shaped patch antenna

The second head imaging antenna also have very less SAR value of 0.0009 W/Kg as shown in figure 4.4

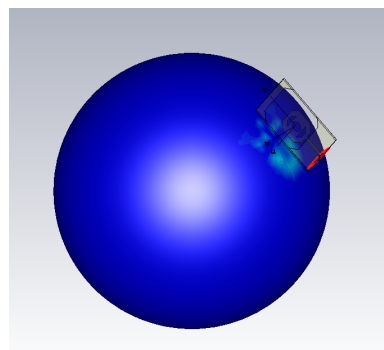


Figure 4.4: SAR analysis of modified square shaped patch antenna



# Chapter 5

## TUMOR DETECTION

### 5.1 ANTENNA INVESTIGATIONS IN DESIGNED PHANTOM ENVIRONMENT

For detecting the presence of tumor we have to place the respective antenna with the designed phantom model. The signals that radiates from the antenna will hits the phantom including the tumor. The radiated signals will be reflected from the phantom would be analysed to prove the presence of tumor. Since each layer or tissue having different permitivitty and conductivity hence the signal that reflected from each tissue will defently operates at different frequency ranges. By analysing this frequency in time domin we can localize the tumor position.

We place the CPW-fed pentagonal patch antenna with the breast phantom. We designed the tumor at the center of the phantom model. The distance between center of antenna to the center of designed phantom is 100 mm as shown in figure 5.1. The S parameter plot of the above is shown in figure 5.2. In this case we vary the distance between center of the antenna to center of phantom vary from 80 mm to 100 mm to get 10 samples. Each plot of sample is given in the figure 5.2

We also placed the second antenna which we have designed, blade shape patch antenna with the breast phantom. We designed the tumor at the center of the phantom model. The distance between center of antenna to the center of designed phantom is 100 mm as shown in figure 5.3. The S parameter plot of the above is shown in figure

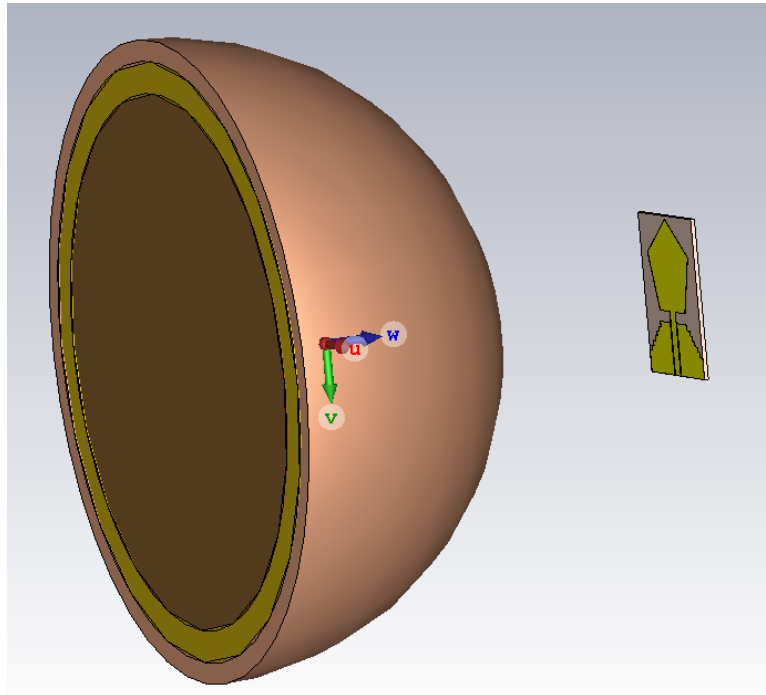


Figure 5.1: CPW-fed pentagonal patch antenna with breast phantom model

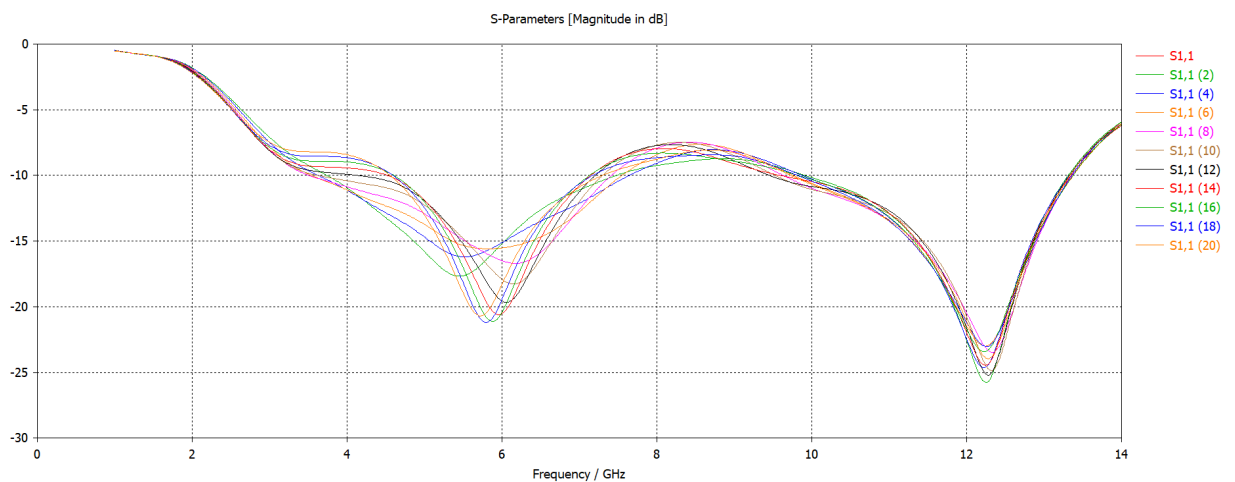


Figure 5.2: S parameter plot of CPW-fed pentagonal patch antenna with breast phantom model

5.4. We conduct a parametric study by varying the radius of tumor from 10 mm to 20 mm to get 5 samples. Each plot of sample is given in the figure 5.3

For detecting the presence of brain tumor we place the flower shaped patch antenna with the designed head phantom model. We designed the tumor at the center of the phantom model. The distance between center of antenna to the center of designed

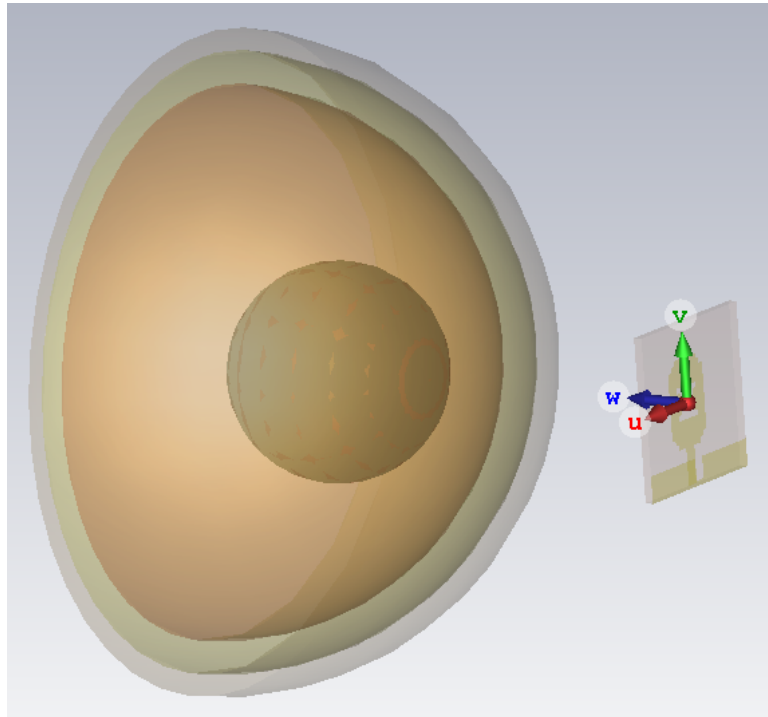


Figure 5.3: Blade shaped patch antenna with breast phantom model

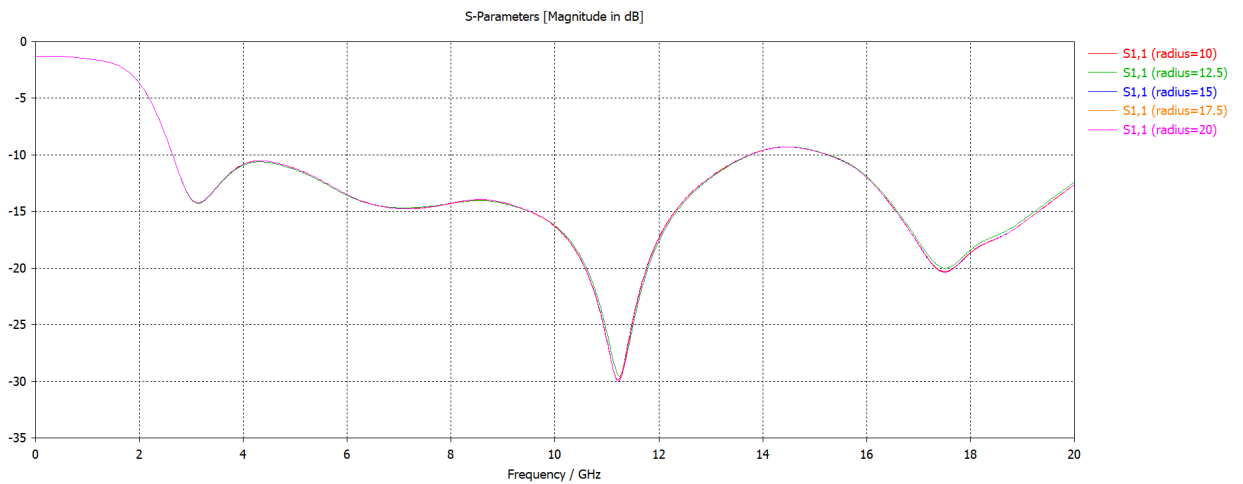


Figure 5.4: S parameter plot of blade shaped patch antenna with breast phantom model

phantom is 150 mm as shown in figure 5.5. The S parameter plot of the above is shown in figure 5.6. We conduct a parametric study by varying the radius of tumor from 15 mm to 25 mm to get 5 samples. Each plot of sample is given in the figure 5.6

And finally we place the modified square shape patch antenna with the head phantom for detecting brain tumor. In this case also the tumor at the center of the

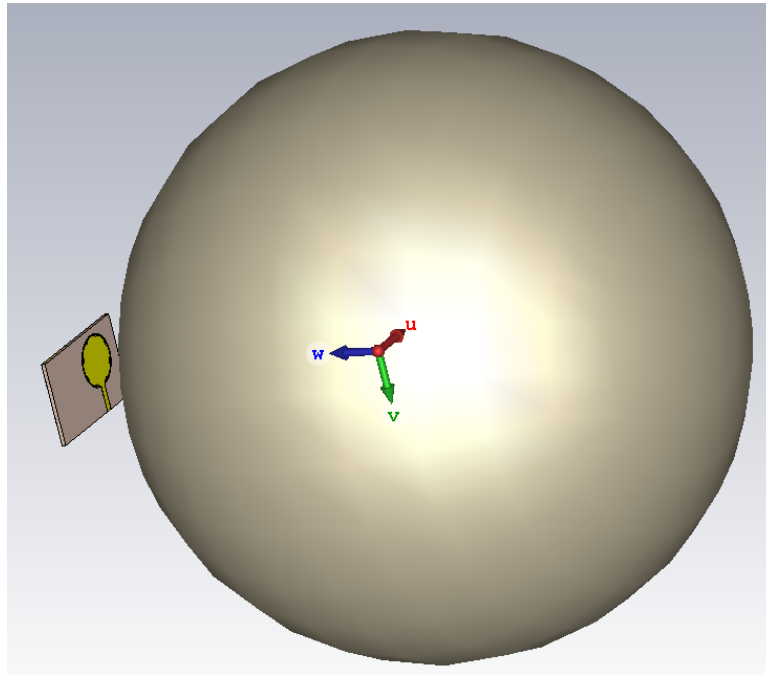


Figure 5.5: Flower shaped patch antenna with head phantom model

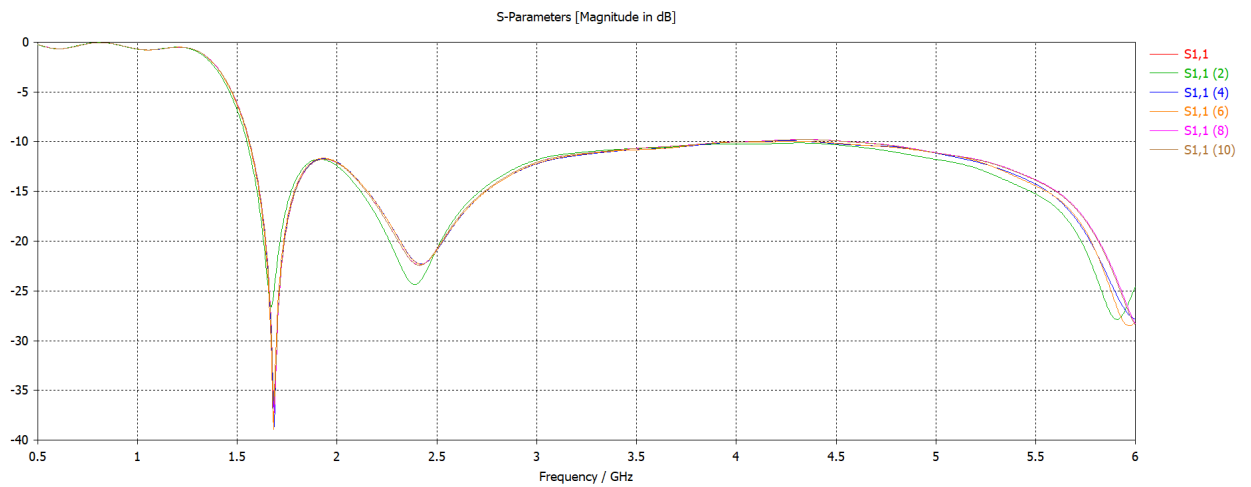


Figure 5.6: S parameter plot of flower shaped patch antenna with head phantom model

phantom model. The distance between center of antenna to the center of designed phantom is 150 mm as shown in figure 5.7. The S parameter plot of the above is shown in figure 5.8. We vary the radius of tumor from 15 mm to 25 mm to get 5 samples. Each plot of sample is given in the figure 5.8

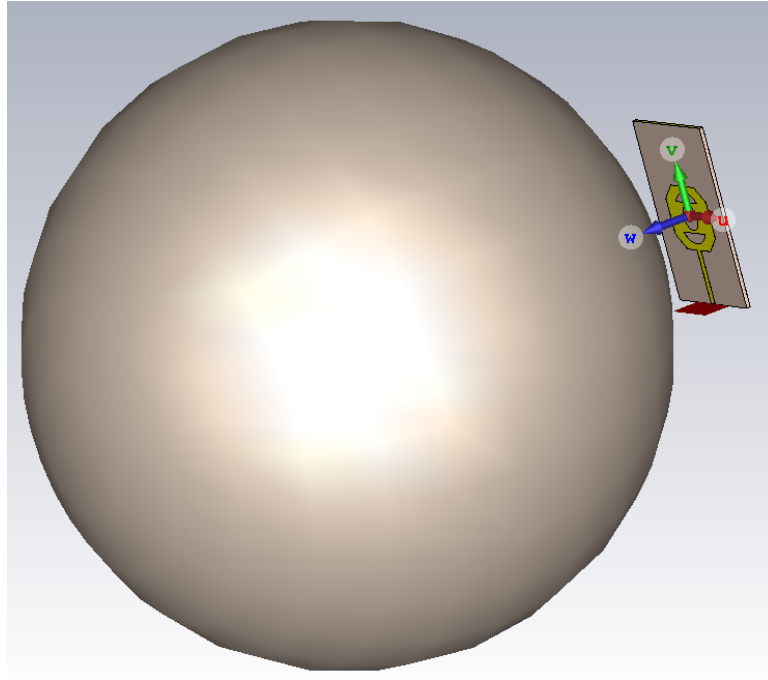


Figure 5.7: Modified square shaped patch antenna with head phantom model

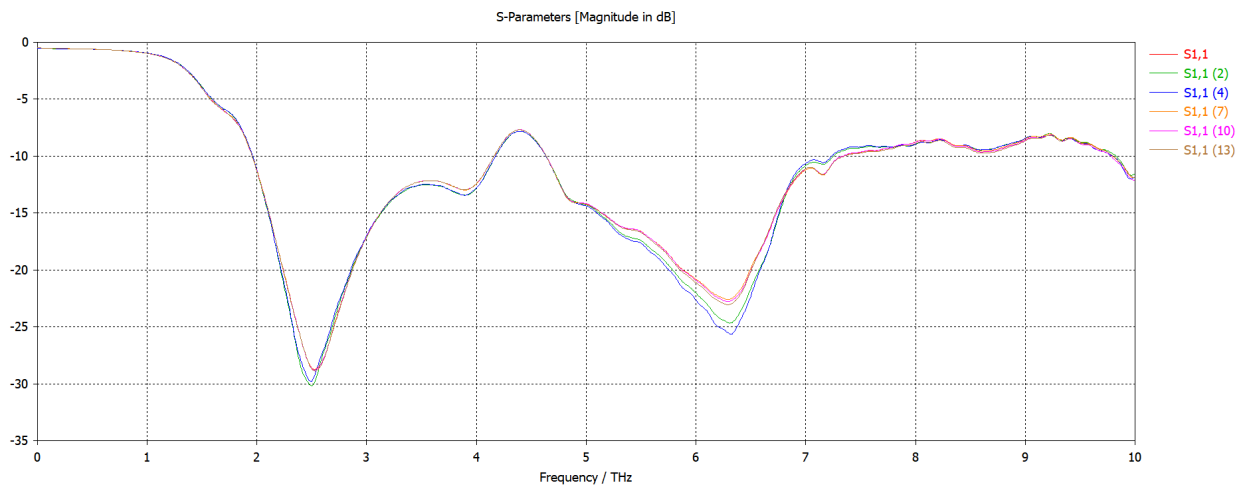


Figure 5.8: S parameter plot of modified square shaped patch antenna with head phantom model

## 5.2 IMAGE RECONSTRUCTION OF TUMOR

The images that obtained by antenna and phantom model are reconstructed using DAS and DMAS algorithm to see the presence of tumor. The frequency domain S parameter plot (figure 5.4) that obtained by antenna and phantom are converted to time domain. Then by using the algorithm the time domain signal will converted to

reconstructed image. Figure 5.9 shows the breast reconstructed image of antenna 3.5 using DAS algorithm and figure 5.10 shows the breast reconstructed image of antenna 3.5 using DMAS algorithm. Each image is normalized to its maximum intensity. The dotted black circle indicates the antenna trajectory during the scan, the dotted white line indicates the approximate breast phantom boundary, and the solid green circle indicates the known tumor position.

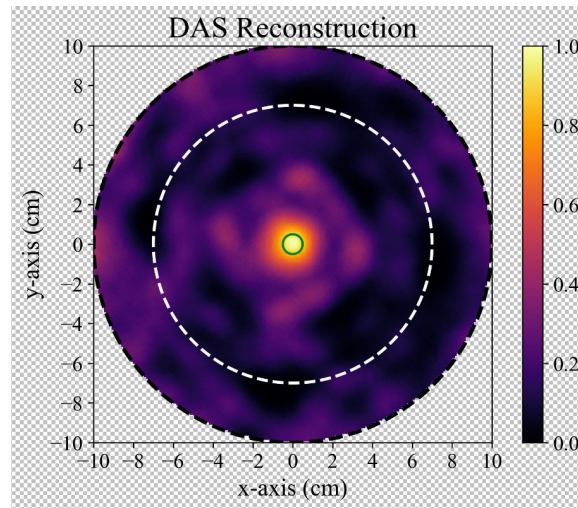


Figure 5.9: Breast image reconstruction using DAS algorithm

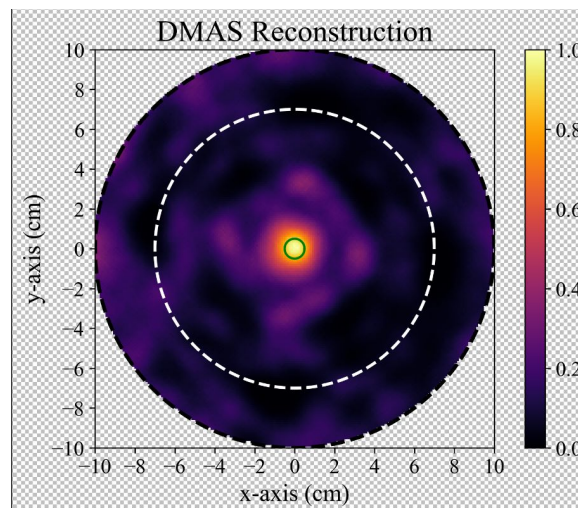


Figure 5.10: Breast image reconstruction using DMAS algorithm

# Chapter 6

## CONCLUSION & FUTURE SCOPE

In this research we designed four UWB patch antennas for tumor detection . Two for breast imaging and two for head imaging. All of them are in UWB frequency range. All the proposed structure functions with impedance matching performance greater than 10 dB and have high fractional bandwidth percentage. All the antenna structure are compact in size and high gain value which is the highest as compared to similar works in literature. By calculating the SAR value, the designed antennas are further examined for its suitability imaging of the human body. The SAR value obtained at multiple frequencies in the frequency range of operation is lower than 1.6 W/Kg, demonstrating that the developed design follows the FCC regulations. All the SAR value are very much less than the acceptable range, hence they are very much safe to use even from home itself. Then we analyse the S parameter plot of antenna with phantom model by varying some parametric values. Finally the obtained S parameter is reconstructed using DAS and DMAS algorithm for tumor localization. The proposed antennas can be used to detect other cancers or fibroids at later stage. As studies suggested the women with hormonal breast cancer have 60% chance to get ovarian cancers or fibroids [1-6]. Hence we can detect these using the proposed antennas. Also we can use multistatic approaches at later stage for more accurate results.

## Chapter 7

# PUBLICATIONS FROM THIS THESIS

- Athul O Asok, **Anjaly R**, Nissan Kunju, Sukomal Dey, “Monopole Antenna Loaded With Wind Mill Shaped FSS For Breast Tumor Detection”-International Conference on Microwave Antenna and Communication(MAC 2023) March 24-26,2023, Jointly Organised by MNNIT ALLAHABAD, India, Universite de Sherbrooke, Canada and Benedict College, Columbia, USA, Proceedings will be published in IEEE Xplore Digital Library, ( Presented )
- Athul O Asok, **Anjaly R**, Nissan Kunju, Sukomal Dey “Microwave Medical Imaging Using a Compact Monopole Antenna for Brain Cancer Detection”-International Conference on Microwave Antenna and Communication(MAC 2023) March 24-26,2023, Jointly Organised by MNNIT ALLAHABAD, India, Universite de Sherbrooke, Canada and Benedict College, Columbia, USA, Proceedings will be published in IEEE Xplore Digital Library, ( Presented )

# REFERENCES

- [1] Cancer.net, “Breast Cancer - Statistics,” Cancer.net, Feb. 28, 2019. <https://www.cancer.net/cancer-types/breast-cancer/statistics>
- [2] Zerrad, F.-e.; Taouzari, M.; Makroum, E.M.; Aoufi, J.E.; Qanadli, S.D.; Karaaslan, M.; Al-Gburi, A.J.A.; Zakaria, Z. “Microwave Imaging Approach for Breast Cancer Detection Using a Tapered Slot Antenna Loaded with Parasitic Components”. *Materials* 2023, 16, 1496. <https://doi.org/10.3390/ma16041496>
- [3] Mehrotra R, Yadav K. Breast cancer in India: Present scenario and the challenges ahead. *World J Clin Oncol.* 2022 Mar 24;13(3):209-218. doi: 10.5306/wjco.v13.i3.209. PMID: 35433294; PMCID: PMC8966510.
- [4] ] ASCO, “Brain Tumor - Statistics,” Cancer.net, Mar. 20, 2018. <https://www.cancer.net/cancer-types/brain-tumor/statistics>
- [5] Miller, KD, Ostrom, QT, Kruchko, C, Patil, N, Tihan, T, Cioffi, G, Fuchs, HE, Waite, KA, Jemal, A, Siegel, RL, Barnholtz-Sloan, JS. Brain and other central nervous system tumor statistics, 2021. *CA Cancer J Clin.* 2021. <https://doi.org/10.3322/caac.21693>
- [6] National Cancer Institute, “How Cancer Is Diagnosed,” National Can Institute, Jul. 17, 2019. <https://www.cancer.gov/about-cancer/diagnosis>
- [7] Abdul Halim, A.A.; Andrew, A.M.; Mohd Yasin, M.N.; Abd Rahman, M.A.; Jusoh, M.; Veeraperumal, V.; Rahim, H.A.; Illahi, U.; Abdul Karim, M.K.; Scavino, E. Existing and Emerging Breast Cancer Detection Technologies and Its Challenges: A Review. *Appl. Sci.* 2021, 11, 10753. <https://doi.org/10.3390/app112210753>

- [8] Ellingson BM, Wen PY, van den Bent MJ, Cloughesy TF. Pros and cons of current brain tumor imaging. *Neuro Oncol.* 2014 Oct;16 Suppl 7(Suppl 7):vii2-11. doi: 10.1093/neuonc/nou224. PMID: 25313235; PMCID: PMC4195528.
- [9] Karli, Radouane Ammor, Hassan Terhzaz, Jaouad. (2014). Dosimetry in the human head for two types of mobile phone antennas at GSM frequencies. *Open Engineering.* 4. 10.2478/s13531-013-0140-7.
- [10] Kaur, G., Kaur, A. (2020). Breast tissue tumor detection using “S” parameter analysis with an UWB stacked aperture coupled microstrip patch antenna having a “ S ” shaped defected ground structure. *International Journal of Microwave and Wireless Technologies,* 12(7), 635-651. doi:10.1017/S1759078719001442
- [11] Adnan, Shakar Abd-Alhameed, Raed See, Chan Hraga, H. Tamer, Issa Zhou, Dawei. (2010). A Compact UWB Antenna Design for Breast Cancer Detection. *Piers Online.* 6. 129-132. 10.2529/PIERS091029055334.
- [12] Yun, X., E. C. Fear, and R. H. Johnston, “Compact antenna for radar-based breast cancer detection,” *IEEE Trans. Antenna Propagat.,* Vol. 53, 2374–2380, Aug. 2005
- [13] Zerrad, F., Taouzari, M., Makroum, E., Aoufi, J., Nasraoui, H., Aksoy, F.,Islam, M. (2022). Novel measurement technique to detect breast tumor based on the smallest form factor of UWB patch antenna. *International Journal of Microwave and Wireless Technologies,* 1-9. doi:10.1017/S1759078722000289
- [14] Federal communications Commission, Washington, DC, USA, First Report and Order in the Matter of Revision of Part 15 of the Commission’s Rules Regarding Ultra-Wideband Transmission Systems,ET-Docket 98–153, February 2002
- [15] Karli, Radouane Ammor, Hassan Shubair, Raed Alhajri, Mohamed Hakam, A.. (2016). Miniature Planar Ultra-Wide-Band Microstrip Patch Antenna for Breast Cancer Detection. 10.13140/RG.2.2.27536.61448.
- [16] Ponnappalli, Vln Karthikeyan, Shanumugam Narayana, Jammula. (2022). A CIRCULAR SLOTTED SHAPED UWB MONOPOLE ANTENNA FOR

BREAST CANCER DETECTION. Progress In Electromagnetics Research Letters. 104. 57-65. 10.2528/PIERL22040204.

- [17] Rai, C., Singh, A., Singh, S. et al. Dual-Band and Dual Polarized Inverted Pentagonal Shaped Hybrid Cylindrical Dielectric Resonator Antenna for Wireless Applications. *Wireless Pers Commun* 124, 2121–2139 (2022). <https://doi.org/10.1007/s11277-021-09448-2>
- [18] Gupta A, Reddy S, Gangwar RK. Dielectric resonator antenna array for X-band and microwave imaging applications. *Microw Opt Technol Lett.* 2018;60:960-965
- [19] A. I. Affi, A. B. Abdel-Rahman, A. Allam and A. S. A. El-Hameed, “A compact ultra-wideband monopole antenna for breast cancer detection,” 2016 IEEE 59th International Midwest Symposium on Circuits and Systems (MWS-CAS), Abu Dhabi, United Arab Emirates, 2016, pp. 1-4, doi: 10.1109/MWS-CAS.2016.7870066.
- [20] M. M. Islam, M. T. Islam, M. Samsuzzaman, M. R. I. Faruque and N. Misran. “Microstrip line-fed fractal antenna with a high fidelity factor for UWB imaging applications.” *Microwave and Optical Technology Letters* , vol.57, pp.2580-2585, 2015.
- [21] I. M. Danjuma, M. O. Akinsolu, C. H. See, R. A. Abd-Alhameed and B. Liu, “Design and Optimization of a Slotted Monopole Antenna for Ultra-Wide Band Body Centric Imaging Applications,” in *IEEE Journal of Electromagnetics, RF and Microwaves in Medicine and Biology*, vol. 4, no. 2, pp. 140-147, June 2020, doi: 10.1109/JERM.2020.2984910.
- [22] Bah, M.H., Hong, J.-S. and Jamro, D.A. (2016), UWB patch antenna and breast mimicking phantom design and implementation for microwave breast cancer detection using TIME REVERSAL MUSIC. *Microw. Opt. Technol. Lett.*, 58: 549-554. <https://doi.org/10.1002/mop.29613>
- [23] Y.W. Jin, J.M.F. Moura, and Y. Jiang, Breast cancer detection by time reversal imaging, In: *IEEE Biomedical Imaging: From Nano to Macro, ISBI 2008*, 2008

- [24] E.C. Fear, X. Li, S.C. Hagness, and M.A. Stuchly, Confocal microwave imaging for breast cancer detection: Localization of tumors in three dimensions, *IEEE Trans Biomed Eng* 49 (2002), 812–822
- [25] J. Surowiec, S.S. Stuchly, J.R. Barr, and A. Swarup, Dielectric properties of breast carcinoma and the surrounding tissues, *IEEE Trans Biomed Eng* 35 (1988), 257–263.
- [26] M. Ojaroudi and Ö. A. Civi, “High efficiency loop sleeve monopole antenna for array based UWB microwave imaging systems,” 2016 IEEE International Symposium on Antennas and Propagation (APSURSI), Fajardo, PR, USA, 2016, pp. 1781-1782, doi: 10.1109/APS.2016.7696597.
- [27] M. S. Bin Nesar, N. Chakma, M. A. Muktadir and A. Biswas, “ Design of a Miniaturized Slotted T-Shaped Microstrip Patch Antenna to Detect and Localize Brain Tumor,” 2018 International Conference on Innovations in Science, Engineering and Technology (ICISSET), Chittagong, Bangladesh, 2018, pp. 157-162, doi: 10.1109/ICISSET.2018.8745566.
- [28] Cancer.Net. (2018). Brain Tumor – Statistics. [online] Available at : <https://www.cancer.net/cancer-types/brain-tumor/statistics> [Accessed on Jul. 10. 2018].
- [29] Lak, A. and Oraizi, H., 2013. Evaluation of SAR distribution in six layer human head model. *International Journal of Antennas and Propagation*, 2013
- [30] T. Chowdhury, R. Farhin, R. R. Hassan, M. S. A. Bhuiyan and R. Raihan, “Design of a patch antenna operating at ISM band for brain tumor detection,” 2017 4th International Conference on Advances in Electrical Engineering (ICAEE), Dhaka, Bangladesh, 2017, pp. 94-98, doi: 10.1109/ICAEE.2017.8255334.
- [31] M. Woźniak, A. Durka, M. Bugaj, R. Przesmycki, L. Nowosielski and M. Wnuk, “Designing and optimization of microstrip rectangular patch antenna to work on human body,” 2012 19th International Conference on Microwaves, Radar Wireless Communications, Warsaw, 2012, pp. 752-756.

- [32] M. J. Dishali, K. M. Kumar, S. Nawaz, "Design of microstrip patch antenna for brain cancer detection," 2019, ICTACT Journal on Microelectronics - Volume 5 Issue 2
- [33] D. O. Rodriguez-Duarte, J. A. T. Vasquez, R. Scapaticci, L. Crocco and F. Vipiana, "Brick-Shaped Antenna Module for Microwave Brain Imaging Systems," in IEEE Antennas and Wireless Propagation Letters, vol. 19, no. 12, pp. 2057-2061, Dec. 2020, doi: 10.1109/LAWP.2020.3022161.
- [34] M. Rokunuzzaman, A. Ahmed, T. C. Baum and W. S. T. Rowe, "Compact 3-D Antenna for Medical Diagnosis of the Human Head," in IEEE Transactions on Antennas and Propagation, vol. 67, no. 8, pp. 5093-5103, Aug. 2019, doi: 10.1109/TAP.2019.2908066.
- [35] Dobsícek Trefná H, Vrba J, Persson M. Evaluation of a patch antenna applicator for time reversal hyperthermia. Int J Hyperthermia. 2010;26(2):185-97. doi: 10.3109/02656730903436434. PMID: 20146572.
- [36] Md. Mottahir Alam, Md Siam Talukder, Md Samsuzzaman, Asif Irshad Khan, Navin Kasim, Ibrahim Mustafa Mehedi, Rezaul Azim, W-shaped slot-loaded U-shaped low SAR patch antenna for microwave-based malignant tissue detection system, Chinese Journal of Physics, Volume 77, 2022, Pages 233-249, ISSN 0577-9073,
- [37] A. T. Mobashsher and A. M. Abbosh, "Compact 3-D Slot-Loaded Folded Dipole Antenna With Unidirectional Radiation and Low Impulse Distortion for Head Imaging Applications," in IEEE Transactions on Antennas and Propagation, vol. 64, no. 7, pp. 3245-3250, July 2016, doi: 10.1109/TAP.2016.2560909.
- [38] S. A. Kadir Al-Nahiun, F. Mahbub, R. Islam, S. B. Akash, R. R. Hasan and M. A. Rahman, "Performance Analysis of Microstrip Patch Antenna for the Diagnosis of Brain Cancer Tumor using the Fifth-Generation Frequency Band," 2021 IEEE International IOT, Electronics and Mechatronics Conference (IEMTRONICS), Toronto, ON, Canada, 2021, pp. 1-6, doi: 10.1109/IEMTRONICS52119.2021.9422503.